DIPLOMARBEIT

Titel der Diplomarbeit

„Nrf2 activators from nature /

Screening and investigation of a potential crosstalk

between Nrf2 and AMPK"

verfasst von

Johannes Baldinger

angestrebter akademischer Grad

Magister der Pharmazie (Mag.pharm.)

Wien, 2013

Studienkennzahl lt. Studienblatt:	A 449
Studienrichtung lt. Studienblatt:	Diplomstudium Pharmazie
Betreut von:	Univ.-Prof. Dr. Verena Dirsch

Abstract:

Nuclear factor (erythroid-derived 2)-like 2 (Nrf2) is a major transcription factor involved in the defense against cellular stress, and well known for playing a crucial role in homeostasis of a cell. A multitude of positive effects such as antitumor, antioxidant, anti-inflammatory activities, even prolonged live span have been linked to activation of Nrf2. Recent studies also implicate its effectiveness against metabolic diseases like diabetes mellitus type 2, tumorigenesis or liver steatosis. Therefore, activators of Nrf2 may be promising drug candidates for alleviating or preventing these diseases. AMP-activated protein kinase (AMPK) is a master switch in cellular regulation of metabolism and responsive to the AMP/ATP ratio. Activation of AMPK is linked with multiple beneficial effects such as reduced hyperglycemia, increased fatty acid oxidation, reduced inflammation, reduced redox stress or reduced proliferation. These activities partly overlap with the outcome of Nrf2 activation.

In this work we first focused on extracts of five different plants that are used as traditional medicine in Latin America against obesity and/or inflammation. They were screened in a reporter gene assay for Nrf2 activation in order to possibly find novel Nrf2 activators or to provide a molecular explanation for the traditional use of the plants. However, none of the tested extracts showed promising Nrf2 activation.

Secondly we examined a potential crosstalk between Nrf2 and AMPK. We set out to investigate whether the Nrf2 activator Xanthohumol (XN) a prenylated chalconoid found in *humulus lupulus* and furthermore in beer, is able to activate Nrf2 in an AMPK-dependent manner. For this we checked expression of HO-1 (as exemplary Nrf2 target gene) in WT and AMPK ko cells after XN exposure. XN induced HO-1 over time in a strictly Nrf2-dependent manner, an effect that was enhanced when AMPK was present. Presence of AMPK raised both HO-1 mRNA (assessed by qRT-PCR) and HO-1 protein (assessed by Western Blot) expression in XN-treated cells, indicating a positive influence of AMPK at a step prior to transcription of HO-1. Looking for the mechanism underlying the apparent activation of AMPK by XN, we were not able to observe changes in cellular ATP levels (assessed by a luminescence-based assay). But we saw increased mitochondrial superoxide levels in cells treated with XN, which could indicate an impaired mitochondrial electron transport chain. Overall, there is crosstalk between Nrf2 and AMPK in XN-treated cells. The detailed molecular mechanisms need further investigation.

Zusammenfassung:

Nuclear factor (erythroid-derived 2)-like 2 (Nrf2) ist ein Transkriptionsfaktor, der neben Adenosin Monophosphat aktivierter Proteinkinase (AMPK) den Mittelpunkt dieser Arbeit darstellt.

Nrf2 wird durch oxidativen Stress aktiviert und führt zu gesteigerten Expressionsraten einer Vielzahl von Phase II Entgiftungs-Proteinen wie Hämoxygenase 1 (HO-1). Die Aktivierung von Nrf2 induziert antioxidative, antientzündliche und in weiterer Folge antitumorale Mechanismen. Somit ist Nrf2 ein wichtiger Bestandteil der Zelle im Kampf gegen zellulären Stress. Oxidativer Stress bzw. Entzündungen beeinflussen metabolisch bedingte Erkrankungen wie Diabetes mellitus Typ 2 oder Lebersteatose nachweislich negativ, daher könnten Nrf2 aktivierende Stoffe ein vielversprechendes Arzneimitteleinsatzgebiet zur Vorbeugung bzw. Linderung dieser Krankheiten darstellen.

AMPK ist entscheidend am Energiehaushalt einer Zelle beteiligt und reagiert auf Änderungen im AMP-/ATP-Verhältnis. Aktivierte AMPK steht in Verbindung mit einer Vielzahl von positiven Eigenschaften wie z.B. Reduzierung von Hyperglykämie, gesteigerter Fettsäure Oxidation, Verringerung von Entzündungsprozessen, reduziertem Redox Stress und verminderten Zellteilungsraten. Aktivierte AMPK hat somit auch antikanzerogene Effekte.

Aufgrund sich überschneidender Eigenschaften ist eine gegenseitige Beeinflussung von AMPK und Nrf2 in Betracht zu ziehen.

Erstes Ziel dieser Arbeit war es, die Aktivierung von Nrf2 durch Extrakte aus fünf unterschiedlichen Pflanzen auszutesten, um dabei neue potentielle Nrf2-Aktivatoren zu erhalten. Es handelte sich dabei um Pflanzen, die in der lateinamerikanischen Volksmedizin gegen Fettleibigkeit und Entzündungen eingesetzt werden. Keines der getesteten Extrakte zeigte schlussendlich die vermutete Nrf2-Aktivierung.

Ein weiterer Fokus dieser Arbeit lag auf der Untersuchung der Interaktion von Nrf2 und AMPK. Es wurde mit Xanthohumol (XN), ein prenyliertes Chalkon aus *Humulus lupulus*, gearbeitet, welcher Nrf2 aktiviert.

Durch die Wiederholung vorangegangener Experimente wurde bewiesen, dass XN in Maus embryonalen Fibroblasten (MEF) die HO-1-Expression antreibt. Hingegen wurden in Nrf2 ko Zellen keine und in AMPK ko Zellen nur verminderte HO-1 Spiegel produziert. Demzufolge ist die HO-1-Expression streng Nrf2 abhängig, wobei in Anwesenheit von AMPK eine zusätzliche Steigerung der HO-1-Expression stattfindet.

In einem weiteren Experiment wurde durch quantitative Echtzeit polymerase Kettenreaktion (qRT-PCR) von HO-1 mRNA festgestellt dass AMPK seinen Einfluss auf Nrf2 bereits zum Zeitpunkt der Transkription ausübt.

Weitere Untersuchungen sollten zeigen, welche spezifischen Mechanismen durch AMPK ausgelöst werden und somit zu einer gesteigerten Nrf2-Aktivität führen.

Dazu wurde mit der Nrf2 aktivierenden Substanz XN in MEF-Zellen ein Lumineszenz Assay durchgeführt, um sich ändernde ATP-Spiegel festzustellen. Die Ergebnisse waren jedoch nicht signifikant.

Im letzten Versuch dieser Arbeit testete man mittels XN stimulierten MEF-Zellen im Zuge einer Durchflusszytometrie auf sich ändernde Superoxid-Spiegel. In den Ergebnissen zeigte sich, dass XN die in den Mitochondrien stattfindende oxidative Phosphorylierung unterbricht. Es kommt daher einerseits zu gesteigerten Superoxid-Spiegeln und anderseits zu Änderungen in den ATP-Vorräten der Zelle. Ob dieser Effekt jedoch für die zusätzliche Aktivierung von Nrf2 durch AMPK verantwortlich ist, bleibt weiters unbekannt.

A) Contents

A) Contents

x

B) Introduction

B) Introduction

In the following section the three main players of this work are briefly introduced: Nuclear factor (erythroid-derived 2)-like 2 (Nrf2), AMP-activated kinase (AMPK) and xanthohumol (XN).

B.1 NRF2

Nuclear factor (erythroid-derived 2)-like 2 (Nrf2) is a transcription factor and an important protagonist in the cellular defense mechanism against oxidative and xenobiotic stress.

Nrf2 belongs to basic leucine zipper transcription factors and is a member of the cap'n'collar family, such as Nrf1, Nrf3, Bach1 and Bach2 do. These molecules comprise the cell's major answer to stress induced by endo- or exogenous factors such as heavy metals, electrophiles or ROS [1]

B.1.1 NRF2- THE WAY IT WORKS.
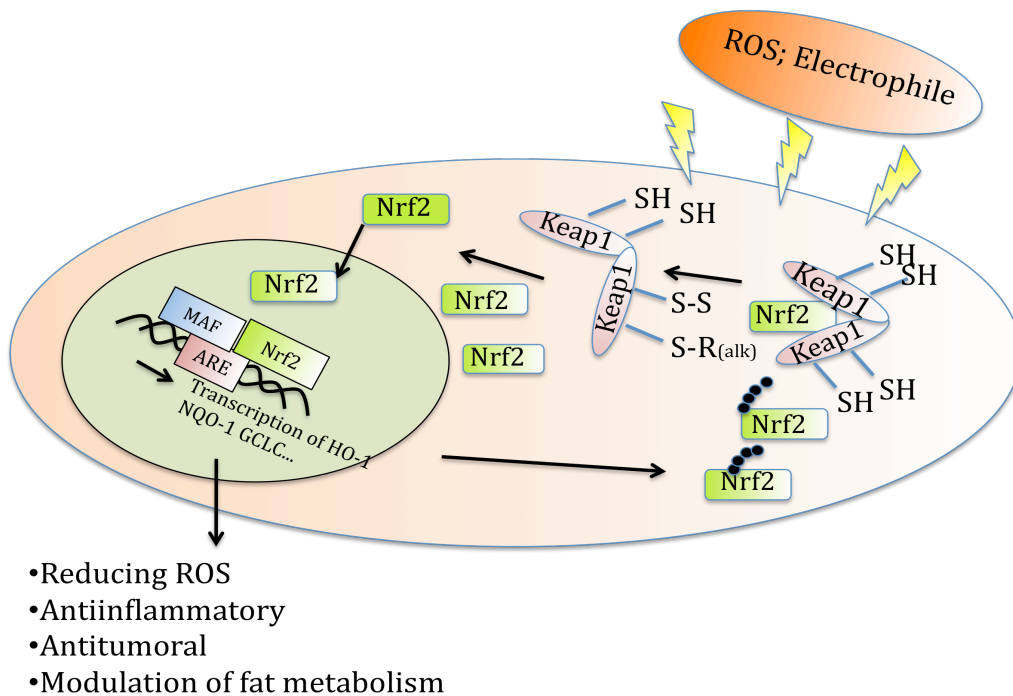
Figure 1) Nrf2 pathway: ROS or electrophiles are inducing stress in a cell, causing oxidation/covalent modification of Keap1 thiol residues. The resulting conformational change within Keap 1 molecules releases Nrf2 and thus stops degradation of Nrf2. If the concentration of Nrf2 in the cytosol is reaching a certain concentration, it enters the nucleus where it binds to MAF and then to ARE consensus region on the DNA. Transcription of Nrf2 target genes is initiated.

Nrf2 is in its inactive state bound to its inhibitor Keap1 which remains in the cytosol and mediates constant proteasome-dependent degradation of Nrf2. Nrf2 interacts with two Keap1 molecules (Kelch like ECH-associated protein 1) via its Neh2 domain [2] which possesses two binding sites, a high affinity site called ETGE and a low affinity site called DLG for Keap1 [3]. Keap1 is an adapter for Cullin3 (Cul3) ubiquitin E3 ligases that mediates ubiquitination and thus proteasome-dependent degradation of Nrf2 [4]. The depletion of Nrf2 is performed in about 15-20 minutes, a very fast process [5].

Keap1 is rich in cysteine residues that act as sensors for oxidative and xenobiotic stress: If cellular stress occurs, thiol residues of Keap1 are modified, leading to a conformational change. Hereby Nrf2 is released from Keap1 and from proteasomal degradation and at a certain threshold concentration it migrates into the nucleus. There it heterodimerizes with musculoaponeurotic fibrosarcoma (MAF) and binds to its DNA consensus region of ARE (antioxidant response elements) in order to start the transcription of Nrf2 target genes including phase II detoxifying and cytoprotective proteins like nicotinamid adenine dinucleotide phosphate (NAD(P)H), nicotinamid adenine dinucleotide phosphate dehydrogenase quinon 1 (NQO1), heme oxygenase (HO-1), glutamate - cysteine ligase catalytic subunit (GCLC) etc. [6].

B.1.2 THE NRF2 PATHWAY AS DRUG TARGET

Due to its spectrum of protective target genes Nrf2 has been extensively investigated in the context of prevention and/or treatment of diseases which are associated with oxidative stress or inflammation. It was hereby observed that activation of Nrf2 – be it by small chemical entities or by genetic knockdown of Keap1- can confer beneficial effects in several *in vivo* or *in vitro* models of neurodegenerative disease (multiple sclerosis, Alzheimer or Parkinson's disease) [7] atherosclerosis [8], diabetes [9] and obesity [10]. Moreover, activation of Nrf2 appeared for long as a promising strategy to prevent the onset of cancer due to increased detoxification of carcinogens and reduced oxidative damage [11] [12]. However, in recent years it also became evident that Nrf2 activation may be a double-edged sword in the field of cancer. Next to prevention of carcinogenesis activated Nrf2 can also provide some benefit for already existing tumors. Tumor cells with overactive Nrf2, mostly caused by mutation in the Keap1 gene [12], profit from accelerated detoxification of chemotherapeutics, reduced redox stress despite excessive proliferation and a metabolic program that optimally suits their needs [13] [14]. Overall it seems that activation of Nrf2 seems to be a good strategy to prevent rather than to treat disease and potential co morbidities. Notably, also many natural products including sulforaphane, resveratrol or curcumin have been reported to activate Nrf2 [15].

B.2 AMPK

B.2.1 STRUCTURE OF AMPK

AMPK is generally found in the cytosol [16] and composed of a catalytic α-, and the regulatory β- and γ-subunits [17].

α-Subunit

The α-subunit is composed of the catalytic Ser/Thr kinase domain, a β-subunit-binding site, and an AID, ie. an auto inhibitory domain.

Phosphorylation of Thr 172 in the kinase domain causes a strong rise of activity of this enzyme by a factor of 100 fold [18].

It remained unclear for long which kinases are specifically responsible for phosphorylation of the Thr172 residue. After multiple studies it became clear that liver kinase B1 (LKB1), Ca^{2+}-dependent calmodulin-activated protein kinase (CaMKKβ) as well as transforming growth factor beta-activated kinase 1 (TAK1) are responsible for this process [19].

β-Subunit

This subunit is made up of a glycogen-binding site, which mediates binding of AMPK to glycogen molecules, and on its C-terminal end there is an α-, γ-subunit-binding site, which enables the three subunits of AMPK to assemble.

γ-Subunit

This subunit contains four cystathionine β-synthase domains (CBS domains), which are crucial for sensing and responding to the cellular AMP/ATP ratio [19]. The four CBS domains form two binding sites for AMP. After AMP has bound to the γ-subunit, a conformational change is taking place, which leads to a moderate increase in enzymatic activity of the holoenzyme. Moreover, the change in conformation favors phosphorylation whilst reducing the chance of dephosphorylation at Thr172 of the α-subunit, which finally massively increases catalytic activity [20].
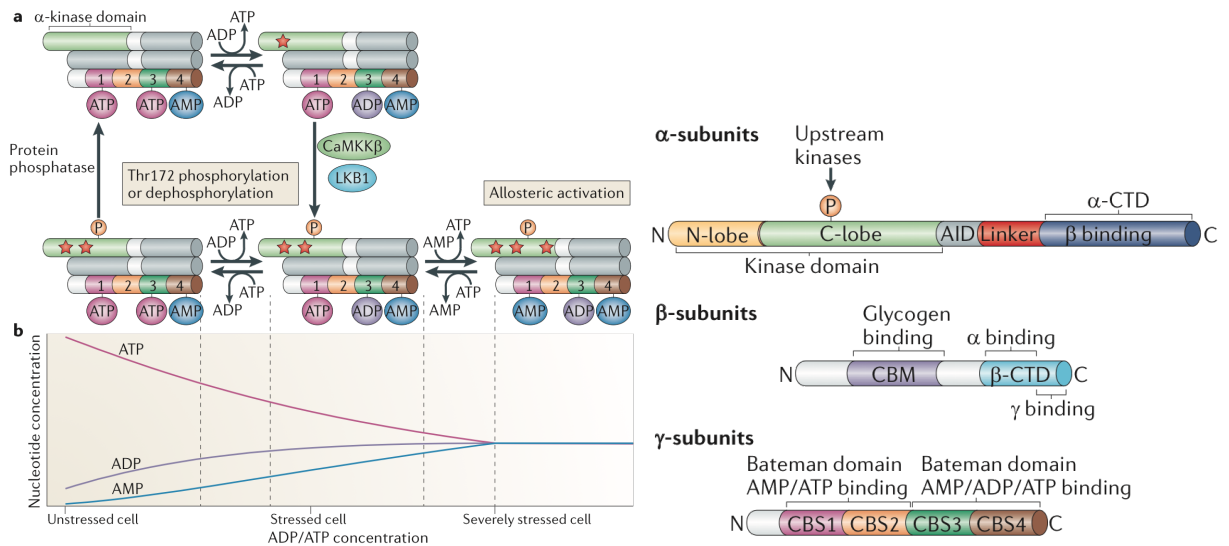
Figure 2) on the left **a)** shows α-,β- and γ-domains, where ATP, ADP and AMP are bound. Furthermore it is pointed how CaMKKβ, LKB1, and the lack of ATP do activate AMPK. **b)** Indicates how falling ATP levels, and therefore altered AMP and ADP levels behave. It is also possible to see that levels of ATP are considerably higher than AMP ADP ratios.

   On the right α-,β- and γ-subunit in greater detail. The important upstream domain of α subunit is pictured. Underneath showing β-subunit with its glycogen -and α-, β-binding site. At the bottom μ-subunit with its important 4 CBS1, 2, 3, 4 domains who are responsible for binding and transforming AMP to ATP [21].

B.2.2 FUNCTIONS OF AMPK
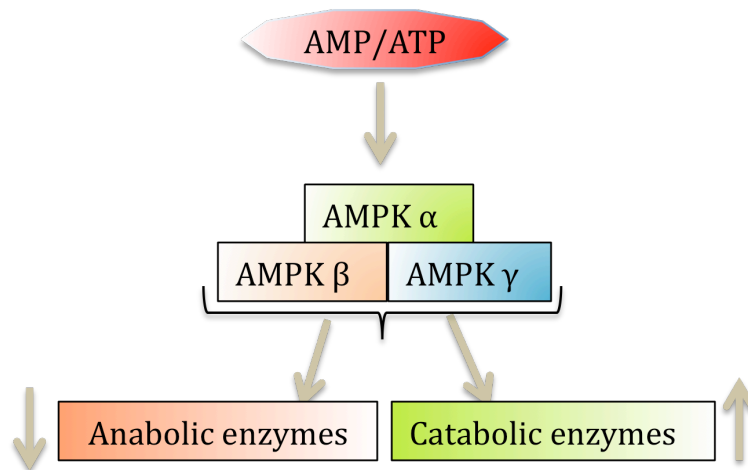
Figure 3) showing major functions of AMPK if AMP/ATP levels rise in favor of AMP, AMPK is activated leading to increased activity of catabolic enzymes and decreased activity of anabolic enzymes, to restore ATP stock again.

AMPK (AMP-activated protein kinase) is ubiquitously found in eukaryotic cells and is predominantly responsible for maintaining sufficient energy equivalents for the cell. It is generally activated in states of low energy (AMP/ATP ratio is high) and leads to activation of catabolic (ATP producing) and inhibition of anabolic (ATP consuming) processes [22]. For

5

example activation of AMPK leads to increased glucose uptake into the cell by increased shuttling of the glucose transporter GLUT4 to the cell membrane [23], shuts down the endogenous production of glycogen (carbohydrates), triglycerides (fats), proteins (amino acids) or cholesterol [24] [25] [26], and increases mitochondrial number and function [27]. The latter activity leads to enhanced physical performance, which has resulted in inclusion of AICAR, an AMPK activator, in the doping list [28]. Next to its direct metabolic activities, AMPK has also been shown to provide beneficial effects against inflammation, redox stress, vascular dysfunction or aberrant proliferation [29] [30] [31]. Interestingly, the outcome of AMPK activation resembles the activity profile of activated Nrf2, possibly indicating that both proteins are members of a common signaling network.

Due to this promising profile elicited by AMPK activation, AMPK arose as a promising drug target. Its activation by small molecules can be obtained by (i) direct binding and inducing a conformational change leading to increased activity, (ii) elevating the AMP/ATP ratio (via mild inhibition of the ATP synthase or interference with mitochondrial respiration) or (iii) by increasing phosphorylation of Thr172 of the α-subunit (e.g. by increasing intracellular Ca^{2+}-levels and CaMKKβ activity) [32].

B.3 Xanthohumol
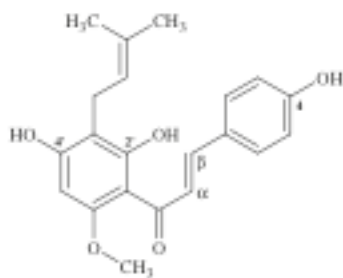
Figure 4) Showing Xanthohumol structure **[34]**

Xanthohumol (XN) is found in hops (Humulus lupulus) and therefore also in beer in a concentration of 0.08 +/ - 0.03 mg/l [33].

Chemically seen it is a prenylated chalcone which shows bad solubility in water. Xanthohumol shows antitumor, antioxidative, antiinflamatory, antiproliferative, antiviral, chemopreventive and antifungal activities in multiple cell-based and *in vivo* studies [34] [35] [36] [37] [38]. The observed effect of XN is very much influenced by the used dose/concentration or model system.

In this study we make use of XN as known Nrf2 activator [39].

B.4 Screening for Nrf2 activators from selected natural sources

B.4.1 SELECTED HERBS AND THEIR EXTRACTION

In order to find potential novel activators of Nrf2, we screened
different extracts of four plants that were kindly provided by B. Theiler and ao. Univ.-Prof.
Mag. Dr. Sabine Glasl-Tazreiter, Department of Pharmacognosy, University of Vienna. These
plants are currently investigated in a project focusing on traditionally used folk medicine to
treat symptoms of diabetes. The plants were *Prunella vulgaris, Leonurus sibiricus, Leonurus
cardiaca* and *Justicia secunda.*

Prunella vulgaris:
 is found in Eurasia and is also widely spread in North America. It is traditionally used for
wound healing and to stop internal bleedings. Extracts of this plant also show antioxidant
potential [40]. Of note, an ethanol extract of *Prunella vulgaris* showed upregulation of HO-1
due to activation of Nrf2 in septic mice [41]. Moreover, a water extract of PV exerted an in
vitro anti-inflammatory effect via inhibition of the ROS/NF-κB pathway by inducing HO-1 and
eNOS expression mediated by Nrf2 [42].
Already isolated constituents from *Prunella vulgaris* include betulinic acid, ursolic acid, 2α,
3α-dihydroxyurs-12-en-28-oic acid and 2α-hydroxyursolic acid [43].

Leonurus sibiricus:
an evergreen shrub belongs to the family of labiatae. Its origin is found in Asia, America and
Africa. For agricultural uses it is mostly grown in Bangladesch, India, China and Myanmar
[44]. This plant has been used in traditional mongolian medicine for 2500-3000 years. The
indications of use are: roots to stimulate respiration, leaves for uterus contraction and chronic
rheumatism, the dried plant is used as a tonic, whilst the seeds are used as an aphrodisiac.
Moreover, also antibacterial effects has been measured [45].

Leonurus cardiaca:
Originally this plant was found in central Europe and Scandinavia and in some regions in
Russia and central Asia, but was later also introduced to North America.
Extracts of this plant are traditionally used against nervous heart conditions, digestive
problems, asthma, climacteric symptoms, amenorrhoea and superficial wounds and skin
inflammations. Also anti-, -oxidant, -inflammatory and analgetic properties are reported [46].

Known constituents are flavonoids, mono-,di-,tri-terpene, phenylpropanoide, nitrogen containing compounds, phenolic acids, essential oils, sterols and tannins.

Justicia secunda:

Justicia secunda belonging to the family of anthaceae is used in the northeastern region of Venezuela. Traditionally it is used as antipyretic, antiseptic and against chicken pox. Other cultures do use parts of the plant or even the whole plant to produce extracts as an infusion against diabetes or amenorrhoea.

Main active agents are lignans and arylnaphthalide [47].

B.5 Aim of the study

This thesis can be roughly divided into two parts.

In part 1 we screened selected plant extracts for their potential to activate Nrf2 using an ARE-dependent luciferase reporter gene assay. These studies were aimed at discovering new Nrf2 activators or at providing a possible molecular explanation for the use of these plants in traditional medicine.

In part 2 we investigated - based on the partly overlapping outcome of Nrf2 and AMPK activation and previous results in our group - the potential crosstalk between these two proteins in the cell. We employed XN as Nrf2 activator and compared the Nrf2-response in wild type mouse embryonic fibroblasts (MEF) and AMPKα ko MEF. The readout for Nrf2 activation was induction of HO-1.

C) Materials and Methods

C) Materials and Methods

C.1 CELL CULTURE

C.1.1 MATERIAL

Name	Provider
Light Microscope Olympus CKX 31	Olympus Europe GmBH (Hamburg, Germany)
Vi-Cell™ XR Cell Viability Analyzer	Beckman Coulter (Fullerton, CA, USA)
HERAsafe™KS Workbench	Thermo Fisher Scientific Inc. (Waltham, CA, USA)
HERAcell™150 Incubator	Thermo Fisher Scientific Inc. (Waltham, CA, USA)
Heraeus™ Multifuge™ 1 S-R Centrifuge	Thermo Fisher Scientific Inc. (Waltham, CA, USA)
Galaxy Mini Microcentrifuge	Thermo Fisher Scientific Inc. (Waltham, CA, USA)
Vortex Shaker	VWR International Inc. (West Chester, PA, USA)
Heraeus™ B15 Incubator KA™	Laboratory equipment (Staufen, Germany)
Eppendorf Pipettes	Eppendorf Austria GmbH (Vienna, Aut)
0.5-10 ml; 1-10 ml; 2-20 ml; 10-1000 ml;	
500-5000 ml; multichannel 10-100 ml	

Consumables

Name	Provider
Serological Pipettes (1 ml, 2 ml, 5 ml,	Sarstedt GmbH (Nümbrecht, Ger.)
10 ml, 25 ml)	
Tissue Culture Flask 75 cm^2	Sarstedt GmbH (Nümbrecht, Ger.)
Tissue Culture Dishes (60 mm, 100 mm)	Greiner bio-one (Kremsmünster. Aut)
96-well Microplates transparent	Greiner bio-one (Kremsmünster. Aut)
PP – Test tubes (15 ml, 50 ml)	Greiner bio-one (Kremsmünster. Aut)
Cell scraper	Greiner bio-one (Kremsmünster. Aut)
Eppendorf Eprouvettes 1.5 ml; 0.5 ml	Eppendorf Austria GmbH (Vienna, Aut)

Cell lines

Mouse embryonal fibroblasts (MEF)

Name	Provider
WT and Nrf2 ko	kind gift of T. Kensler, Pittsburgh, USA
WT and AMPK ko	kind gift of B. Voillet, Paris, France

Chinese Hamster Ovary cells (CHO) stably transfested with ARE-luciferase reporter gene

Name	Provider
CHO ARE LUC	kind gift of D. Zhang, Arizona, USA; clones established by K. Zimmermann, Department of Pharmacognosy, University of Vienna

Media, buffers etc.

Reagents	Provider
DMEM Dulbeccos Modified Eagle's Medium	Lonza Group Ltd. (Basel, Switzerland)
Penicillin/streptomycin mixture (10.000 U/ml potassium penicilline/ 10.000 μg/ml sreptomycin sulphate)	Lonza Group Ltd. (Basel, Switzerland)
L-glutamin 200 mM	Lonza Group Ltd. (Basel, Switzerland)
Fetales Bovines Serum	Invitrogen (Carlsbad, CA, USA)
Trypsin	Invitrogen (Carlsbad, CA, USA)

Working Solutions

Solutions	Reagents	
PBS pH 7.4	NaCl	36 g
	Na_2HPO_4	7.4 g
	KH_2PO_4	2.15 g
	H_2O	ad 5000 ml
Trypsin/EDTA in PBS	Trypsin	0.5 g
	EDTA	0.2 g
	PBS	1000 ml
MEF growth medium	DMEM	500 ml
	FBS (heat inactivated) 10 %	
	L-glutamin	2 mM
	Penicillin/Streptomycin	100 U/ml; 100 µg/ml
CHO/ARE-LUC medium	puromycin	4 µg/ml

C.1.2 GENERAL ASEPTIC RULES

To guarantee an aseptic working condition under the laminar a clean lab coat, good body hygiene, no jewellery and trimmed fingernails are needed. Prior to starting work under the hood it is turned on for at least 20 min to ensure a steady air flow. Work surfaces are wiped with hexaquart and then 70 % ethanol for disinfection.

Everything brought into the laminar has to be as sterile as possible. Therefore material such as pipettes or tip boxes are sprayed with 70 % ethanol and only then placed in the laminar flow. Hands are cleaned with ethanol before entering the hood and starting work.

After finishing work, the work place is cleaned up again, i.e. all media bottles, tip boxes etc are removed, the surface is wiped with 70 % ethanol. At the end of the day the laminar is UV-illuminated for 30 minutes.

C.1.3 CELL CULTIVATION

- **Cell passage**

When adherent cells, like the MEFs and CHO cells, became confluent they were passaged, i.e. detached from the bottom and aliquoted into a new culture flask.

Then, the old medium of the cells to be passaged was removed (either by vaccum aspiration or a pipet), cells were washed with PBS, and then, in order to induce detachment 3 ml of trypsin were added (for a 75 cm flask). After 2-5 minutes of incubation at 37 °C and microscopic confirmation of cell detachment, trypsin was neutralized with 7 ml of complete growth medium (serum naturally contains a trypsin inhibitor). Cell concentration in the suspension was analyzed in a ViCell (Beckman Coulter). A new flask was loaded with 20 ml of fresh growth medium and the required amount of cells (see below). Flasks were labeled with the name and the concentration of cells, the date, the number of the passage and the initials of the person doing the work, and finally placed in the incubator.

Seeded cell number for MEF passages:
- 0.5 million cells for 4-6 days
- 1 million cells for 3-4 days
- 2 million cells following passage 1-2 days till confluency

CHO/ARE-LUC cells
- 1 million cells for 4-5 days
- 2 million cells for 3-4 days
- 3-4 million cells for 1-2 days till confluency

- **Cell freezing and thawing**

When there is no need for a specific cell line these cells are conserved in liquid nitrogen at a temperature of -270°C. In general cells are cooled down as slowly as possible to avoid ice crystal growth which could cause cell death. Ideally the temperature is reduced 1°C per hour. The opposite way thawing them is done as quickly as possible, meaning that the temperature difference from -270°C to 37°C should be bridged in a very short period of time.

To freeze cells they first have to be detached from the cell culture bottle and the concentration has to be measured by Vicell® (exact procedure described in cell culture part). Then the medium is aspirated and substituted by freezing medium consisting of sterile filtered FBS with 10 % DMSO. The cell pellet has to be homogenized. Two million are gathered in 2 ml of freezing medium and filled into screwable cryo tubes that are placed on ice. The freezing

process is started by putting the samples into a special freezing container that is filled with isopropanol and stored at -80°C. After 24 hours cells are transferred into liquid nitrogen. There they can be stored long term.

To thaw cells they are retrieved from the liquid nitrogen, and immediately placed into a 37°C warm water bath. As soon as they begin to thaw the freezing medium is neutralized by 1 ml growth medium, and immediately transferred into a 75 cm^2 culture flask that is also loaded with 20 ml growth medium.

C.2 Western Blot Analysis

C.2.1 GENERAL

Western Blotting is a semi quantitative method for detecting level and modification of a specific cellular protein. For this, cells are lysed and proteins extracted, usually by adding a buffer containing detergent and protease inhibitors and subsequent ultrasound sonification. Proteins are then denatured by heat, a reducing agent (mostly a thio-alcohol, such as dithiothreitol or mercaptoethanol) and SDS is added in order to obtain a linear amino acid chain without higher order structure and a constant negative mass/charge ratio. Then proteins are separated by size when migrating through a polyacrylamid meshwork in an electric field to the positive electrode. Separated proteins are then transferred to a membrane, which can be incubated with an antibody, specific for the protein of interest. To make the protein-antibody complex visible, usually a secondary antibody carrying an enzyme or a chromophore is used.
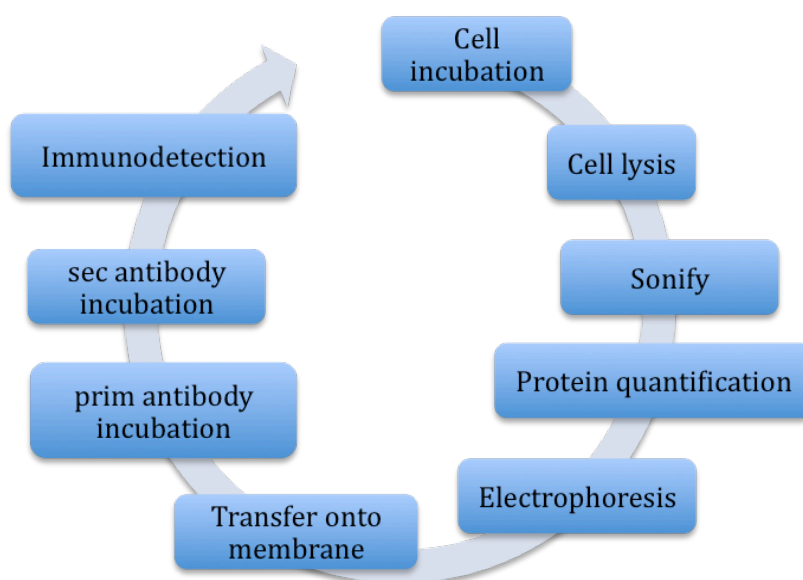
Figure 5) Shows the workflow of Western Blotting.

C.2.2 MATERIAL

Name	Provider
Tecan GENios™Pro, Tecan Sunrise™	Tecan (Mannedorf, Switzerland)
LAS-3000™ Luminescent Image Analyzer	Fujifilm (Tokyo, Japan)
Mini-PROTEAN™ 3 Cell	BIO-RAD Laboratories (Hercules, CA, USA)
Power Pac™ HC power supply	BIO-RAD Laboratories (Hercules, CA, USA)
Mini Trans-Blot™ Electrophoretic Transfer Cell	BIO-RAD Laboratories (Hercules, CA, USA)
HeraeusT™Fresco™ Centrifuge	Thermo Fisher Scientific Inc. (Waltham, CA, USA)
Galaxy Mini Microcentrifuge	Thermo Fisher Scientific Inc. (Waltham, CA, USA)
Vortex Shaker	VWR International Inc. (West Chester, PA, USA)
RCT basic Magnetic Stirrer	VWR International Inc. (West Chester, PA, USA)
Vibrax VXR basic Shaker IKA™	Laboratory equipment (Staufen, Germany)
Bandelin Sono Plus	Bandelin GesmbH (Berlin, Ger.)
Eppendorf Pipettes	Eppendorf Austria GmbH (Vienna, Aut)
0.5-10 ml; 1-10 ml; 2-20 ml; 10-1000 ml; 500-5000 ml; multichannel 10-100 ml	
Dry Block QBD2 2-Bloc system	Grant (Cambridge, UK)

Consumables

Name	Provider
Immun-Blot™ PVDF Membrane (0.2 μm)	BIO-RAD Laboratories (Hercules, CA, USA)
Precision Plus Protein™ Standard	BIO-RAD Laboratories (Hercules, CA, USA)
Gel Blotting Paper	Whatman plc (Kent, UK)
96-well Microplates transparent	Greiner bio-one (Kremsmünster, Aut)
PP – Test tubes (15 ml, 50 ml)	Greiner bio-one (Kremsmünster, Aut)
Eppendorf Eprouvettes 1.5 ml; 0.5 ml	Eppendorf Austria GmbH (Vienna, Aut)

Solutions	Name	Concentration
Lysis Buffer	NaCl	150 mM
Stock solution	Tris-HCl	pH7.450 mM
	Nonidet P 40	1 %
	Deoxycholat	0.25 %
	SDS	0.1 %
	H_2O	ad 50 ml
Before use	Lysis Buffer Stock sol.	1000 µl
	Complete Protease InhibitorMix	
	(Roche)	50 µl
	PMSF (50 mM)	10 µl
Coomassie Blue	Triphenylmethan (5 x)	
Before using	Triphenylmethan (5 x)	1 ml
	H_2O bidest.	5 ml

SDS sample buffer (3 x buffer)

Solution	Reagents	
Stock solution	TRIS-HCL pH 6.8, 0.5 M	37.5 ml
	SDS	6.0 g
	Glycerol	30 ml
	Bromphenol blue	15.0 mg
	Aqua dest.	Ad 100 ml
Before use	Stock solution	85 %
	1,4-Dimercapto-2,3-butandiol	15 %

Electrophoresis gel

Solutions	Reagents	
Stacking gel	PAA 30 %	640 μl
	Tris-HCL 1.25 M pH 6.8	375 μl
	SDS 10 %	37.5 μl
	Aqua bidest.	2.62 ml
	TEMED	7.5 μl
	APS 10 %	37.5 μl
Resolving gel 10 %	PAA 30 %	2.5 ml
	Tris-HCL 1.5 M pH 8.8	1.875 ml
	SDS 10 %	75 μl
	Aqua bidest.	3.05 ml
	TEMED	7.5 μl
	APS 10 %	37.5 μl
SDS 10 %	SDS	5.0 g
	Aqua dest.	ad 50 ml
APS 10 %	APS	1.0 g
	Aqua dest.	ad 10 ml
Complete ™ 25 x	Complete	one tablet
	Aqua dest	2.0 ml
PMSF 0.1 M	PMSF	52.26 mg
	Aqua dest.	ad 3.0 ml
Electrophoresis buffer, 10 x	Tris-base	30 g
	Glycine	144 g
	SDS	10 g
	Aqua bidest.	ad 1000 ml

Before use	Electrophoresis buffer 10 x	100 ml
	Aqua bidest.	ad 1000 ml
Blotting buffer, 5 x	Tris base	15.17 g
	Glycine	72.9 g
	Aqua bidest.	ad 1000 ml
before use:	5 x Blotting buffer	200 ml
	Methanol bidest.	200 ml
	Aqua bidest.	ad 1000 ml
Activation of Membran	Methanol bidest.	q.s.
Blocking solution	TBST	50 ml
	milk powder	2.5 g
ECL solution	Aqua dest.	4.5 ml
	Tris base 1M pH 8.5	0.5 ml
	Luminol	12.5 μl
	p-Coumaric acid	11 μl
	H_2O_2	1.5 μl
Luminol (stock solution)	Luminol	0.44 g
	DMSO	10 ml
p-Coumaric acid (stock solution)	p-Coumaric acid	0.15 g
	DMSO	10 ml
TBS-T pH 8.0	Tris base	3.0 g
	NaCl	11.1 g
	Tween 20	1 ml
	Aqua dest.	1000 ml
	pH was adjusted to 8.0 with HCL conc.	

- **Antibodies:**

Primary antibodies:

Target	Source	Dilution	Producer
Hemeoxygenase	rabbit	1:1000	Stressgen
p-AMPK	rabbit	1:1000	Cell Signaling
tot-AMPK	rabbit	1:1000	Cell Signaling
GCLC	mouse	1:1000	Santa Cruz
GSK3 β	rabbit	1:1000	Cell Signaling
Actin	mouse	1:1000	mpbio
α/β Tubulin	rabbit	1:1000	Cell Signaling

Secondary antibodies (coupled to horse radish peroxidase (HRP)):

Target	Dilution	Producer
Rabbit	1:1000	Cell Signaling
Mouse	1:1000	mpbio

Tested Compounds	Concentrations	Provider
AICAR	(500 µM)	Sigma-Aldrich Co.(St. Louis Missouri USA)
DMSO	(0.1 %)	Sigma-Aldrich Co.(St. Louis Missouri USA)
CDDO-IM	(100 nM)	kind gift of Prof. M.Sporn Dartmouth Med. School USA
Xanthohumol	(5 µM)	Sigma-Aldrich Co.(St. Louis Missouri USA)

C.2.3 PREPARATION OF PROTEIN EXTRACTS

- **Cell incubation**

In order to do our analyses, three different kinds of MEF cells were used: wild type, Nrf2 KO and AMPK KO. To start an experiment cells were seeded into 6 well plates. Usually cells were seeded at a concentration of 300.000 cells per well. After about 12-16 hours of incubation which allowed settling and attachment of the cells, cells were treated as planned. In some experiments cells were seeded at a concentration of 600.000 per well in the morning and incubation was started in the afternoon. Test compounds used were Xanthohumol (XN), an antioxidant in *Humulus lupulus* at a concentration of 5 µM, AICAR, a specific AMPK activator at a concentration of 500 µM and CDDO-IM at 100 nM, a known potent activator of Nrf2. These compounds were given to the cells after changing from medium with 10 % serum to medium with 2 % (in order to reduce serum binding and inactivation of the compounds) and left on the cells for different periods of time as indicated in the results section.

- **Cell lysis**

Cells were placed on ice, and supernatant was taken off. Then MEFs were washed with 2-3 ml of ice cold PBS. After that, 100 µl of lysis buffer was added per well. Cells were scratched from the surface with a cell scraper and transfered in a 1.5 ml reaction tube that was placed on ice.

In order to homogenize the whole cell material and break up all membranes, the lysate was sonified with a bandelin sono plus sonficator using ultrasound at a range from

$16 \text{ kHz} < f < 1 \text{ GHz}$.

10 second pulses with an intensity of 85-90 % were used while the ears were protected from the sound with a headset. Tubes were kept on ice in order to reduce heating of the samples which negatively affects proteins. After sonfication of one sample, the ultrasound tip was rinsed with water.

To get rid of all insoluble particles, samples were centrifuged for 15 min with 13.000 rpm at a temperature of 4°C. The supernatant containing all solubilized proteins was used for further tests or stored at -20°C.

- **Protein quantification**

The next step would be to identify the quantity of proteins in the lysate.

For this, a Bradford assay was performed. First an aliquot of each cell lysate was diluted 1:5 in water, vortexed and centrifuged (overall 50 µl). Then samples at a volume of 10 µl in triplicate

and a standard curve with defined concentrations of bovine serum albumin were pipetted in a 96-well plate. Staining was done with Coomassie blue G-250 (RotiQuant from Carl Roth) that was diluted 1:5 with water before use. 190 µl of the staining solution were added to the samples and standard curve. Coomassie blue interacts with proteins, forming a complex that alters absorption of the dye from 490 nm to 595 nm. The Bradford assay is very sensitive and stable (the staining is kept for about 4 hours). Absorbance readings at 595 nm were performed on a spectrophotometer (TECAN, Sunrise). The protein concentration of the lysates was calculated according to the BSA calibration curve. For a gel, usually 10-20 µg per slot were used.

- **Denaturation**

Before loading on a gel, appropriate amounts of cell lysates were denatured. For this, the lysates were mixed with 3 x SDS sample buffer (volume of the buffer at least ½ x volume of the lysate) and incubated at 95°C for about 5 minutes. After a quick spin, samples were either frozen at -20°C or immediately subjected to electrophoresis.

C.2.4 ELECTROPHORESIS

- **Preparation of the gel**

Gels were usually prepared the day before the run. For this, two glass plates, one flat and the other with a permanent spacer of 1.5 mm, were cleaned and assembled according to the manufacturers instructions (Mini-PROTEAN™ 3 Cell from BioRad).

Resolving gel solution was filled in and covered with isopropanol. After 45 min the gel was polymerized. Isopropanol was removed. After a quick rinse with water, the stacking gel solution was added and finally the comb was set in. After polymerization, the gel was stored at 4°C overnight (or up to 7 days).

- **Gel run**

Gels were placed in the clamping frame. The electrophoresis chamber was loaded with the clamping frame, and filled up with 1 x electrophoresis buffer. The comb was removed and pockets were washed with buffer.

Then, the pockets of the gel were loaded with the denatured protein samples. In addition, 5-7 µl of a molecular weight marker (prestained MW marker from BioRad) were pipetted in one pocket of the gel.

The electrophoresis run was performed at 30 mA for one gel and at 50-60 mA for two gels (power supply: Power Pac™ HC power supply from BioRad). The run was finished when the blue front of the sample buffer had reached the bottom of the gel.

C.2.5 TRANSFER TO THE MEMBRANE

The separated proteins on the gel were now transferred to a PVDF membrane by a wet blotting system from BioRad. Before the membrane was used it was activated in methanol. Foam pads, the filters and the activated membrane were soaked in blotting buffer before use. Blotting sandwich was prepared according to the manufactures instructions. Briefly, the blotting cassette was filled in the following order: a foam pad, a filter, the resolving gel, the membrane, the second filter and finally another foam pad. After careful removal of any air bubbles, the blotting cassette was closed, put in the chamber and filled with 1 x blotting buffer. Further a cooling block and a magnet stirrer were added to guarantee a persistent flow of buffer solution at a steady temperature. The transfer was performed at 100 V for at least 100 minutes.

C.2.6 IMMUNODETECTION

When the transfer was finished, the membrane was removed from the cassette, and free binding sites were blocked with blocking solution for at least 20 min. Meanwhile primary antibody solutions were freshly prepared (mostly 1:1000 dilution in TBS-T) or thawed (primary antibody dilutions can be frozen at -20°C and then be reused for up to 8 times). The membrane was withdrawn from the blocking solution, and washed with TBST three times for 1 minute. Afterwards it was put in primary antibody solution on a constant turning rotor for 1 ½ hrs at room temperature or over night at 4°C. The membrane was then washed three times for 10-15 minutes in TBST and transfered into the secondary antibody solution. This incubation step was usually performed at room temperature for 1-2 hrs. Then the membrane was again washed three times with TBST for 15 minutes.

In order to visualize the protein of interest, a mixture of para-coumaric acid, luminol, ECL buffer, hydrogen peroxide and water (see exact recipe "ECL solution" under 2.2) was added to the membrane. The peroxidase, which is coupled to the secondary antibody, is now able to emit a luminescence signal. This chemoluminescence signal is collected and digitalized by a CCD camera (LAS 300) resulting in a dark signal at the site were the antibodies have bound. The bands can be densitometrically evaluated by the AIDA software.

C.2.7 STRIPPING

When the first immunodetection was done bound antibodies had to be removed to allow unflawed detection of other proteins. Thus the membrane was washed with 0.5 N NaOH solution for 10 minutes. Then it was washed three times with TBS-T for 1 minute. The membrane was ready to be incubated in the next primary antibody solution.

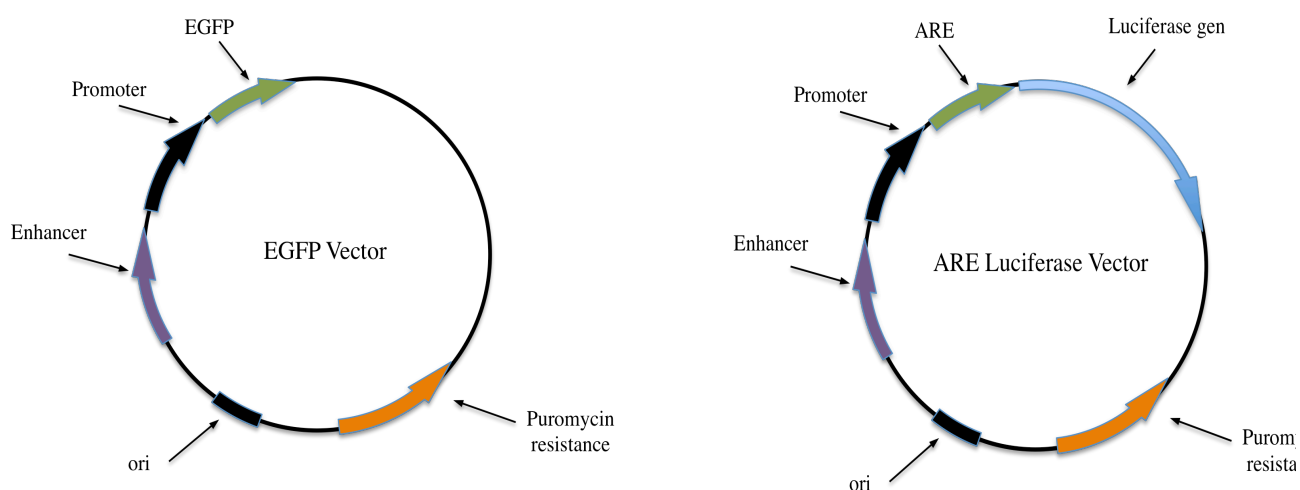## C.3 Luciferase reporter gene assay:

C.3.1 GENERAL

Figure 6) Is showing two plasmids used for transfecting cells. Containing genetic information for EGFP on the left and the ARE-luciferase plasmid on the right. Both plasmids carry puromycin resistance genes. Puromycin is needed to select transfected cells from not transfected.
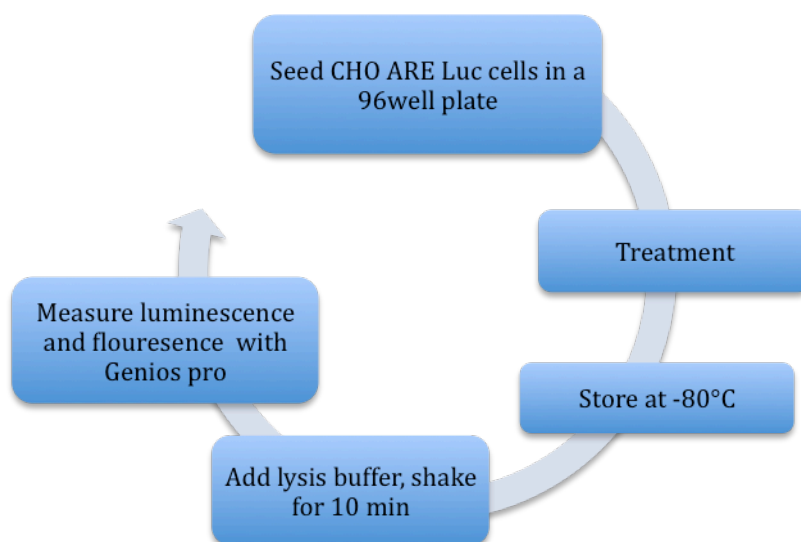

Figure 7) Is showing the workflow of luciferase reporter gene assay.

23

Reporter gene assays usually allow to determine activation or inhibition of a specific transcription factor by coupling the respective response element to a gen whose activity can be easily assessed. In our case, the ARE sequence, which responds to Nrf2 activation, is coupled to luciferase gen. This construct has been stably integrated in the genome of the CHO cells, resulting in CHO/ARE-LUC cells. When these cells are incubated with Nrf2 activators, luciferase is expressed. Luciferase expression can then be quantified in the cell lysates according to the amount of emitted luminescence when luciferin and ATP, substrates of luciferase, are added. This system allows a fast and medium to high-throughput screening for potential Nrf2 activators. To account for cytotoxic events, the cells are furthermore transfected with an expression vector for green fluorescent protein which allows normalization of the inducible luminescence to the constitutive fluorescence values.
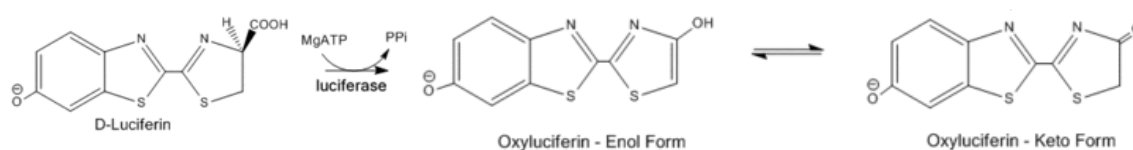

Figure 8 Shows how Luciferin is transformed into Oxyluciferin. This is the step that turns luciferin into a luminescent signal emitter **[48].**

C.3.2 MATERIAL

Name	Provider
Tecan GENios™Pro, Tecan Sunrise™	Tecan (Mannedorf, Switzerland)
Multi-Microplate Genie™	Scientific industries (Bohemia, NY, USA)

Solutions	Reagents	
Lysis buffer (5 x)	Lyse buffer	9.6 ml
Luciferin solution	Luciferin	25 mg
	dd H_2O	8.27 ml
Luciferase buffer	Luciferin solution	1.1 ml
	1 M Tricine buffer (pH 7.8)	220 µl
	dd H_2O	9.2 ml

ATP solution (pH 7.0)	ATP (Sigma)	1 g
	1 N NaOH	3.3 ml
	ddH$_2$O	13.4 ml
Tricine-ATP-buffer	1 M Tricine buffer	220 μl
	0.5 M MgCl$_2$	473 μl
	0.1 M ATP	407 μl
	0.27 M Coenzyme A	10 μl
	dd H$_2$O	9.9 ml
	DTT	11 μl
Lysis buffer	Lyse buffer (5 x)	9.6 ml
	H$_2$O	2.4 ml
	CoA	12 μl (270 mM)
	DTT	12 μl (1M)

- **Used test compounds:**

Name	Concentrations	Provider
CDDO IM		kind gift of Prof. M.Sporn Dartmouth med. School USA
Xanthohumol	5 μM	Sigma-Aldrich St. Louis, MO USA
Aicar	500 μM	Sigma-Aldrich St. Louis, MO USA
DMSO	0.1 %	Sigma-Aldrich St. Louis, MO USA
Chlorophyll:	25 μg/ml	Sigma-Aldrich St. Louis, MO USA

- **Extracts:**

Plant	used part	Extraction solvents	Provider
Prunella Vulgaris:	Leaves	PE, BuOH, H$_2$O, OWE, DCM, MeOH	Barbara Theiler
Justicia secunda:	Leaves	PE, BuOH, H$_2$O, OWE, DCM	Barbara Theiler
Leonurus Cardiaca:	Leaves	MeOH, PE, DCM, BuOH, H$_2$O, OWE	Barbara Theiler
Leonurus Sibiricus:	Leaves	BuOH	Barbara Theiler

C.3.3 PREPARATION OF THE CELLS

CHO cells stably transfected with ARE-LUC reporter and EGFP expression plasmids were seeded into 96-well plates at a concentration of 30.000 cells / well in 100 µl growth medium and left in the incubator for at least 12 hrs.

C.3.4 TREATMENT WITH TEST COMPOUNDS

Compounds and extracts were diluted in DMEM medium without serum to a concentration that was 2 x the wanted test concentration on the cell. From these dilutions, 100 µl were pipetted to the appropriate wells in the prepared 96-well plate with CHO/ARE-LUC cells. Usually each compound or extract was tested at least in quadruplicate.

As positive control CDDO-IM (100 nM) was used. DMSO (0.1 %) served as negative control.

To stop the treatment, which usually was done for 16-24 hrs after addition of the compounds, medium was taken off, cells were washed with PBS and then frozen at -80°C for at least one hour.

C.3.5 GENERATING PLANT EXTRACTS

Table 1 depicts an overview of the plants, the used parts of the plant and extracts tested in this experiment. In general, the principle underlying extraction scheme for each herb was to first extract with methanol, and then to extract with solvents of different polarity, ranging from dichlormethane (CH_2Cl_2) to water. Water extract was done with hot water. Original water extract (OWE) was simulating the conditions in the stomach. So plant material was put in water with a pH of 2.0 at a constant temperature of 37°C for two hours. After extraction, the solvents were evaporated. The remaining powder was dissolved in DMSO and provided at a concentration of 25 mg/ml. The solvents were stored in aliquots at -20 °C.

Plant name	Family	Extract	Used part
Prunella vulgaris	Lamiaceae	MeOH	leaves
		PE	
		CH_2Cl_2	
		BuOH	
		H_2O	
		OWE	
Leonurus sibiricus	Lamiaceae	BuOH	leaves
Leonurus cardiaca	Lamiaceae	MeOH	leaves
		CH_2Cl_2	
		BuOH	
		H_2O	
		OWE	
		PE	
Justicia secunda	Acanthaceae	CH_2Cl_2	leaves
		BuOH	
		H_2O	
		OWE	
		PE	

Table 1) Overview of tested plant extracts.

C.3.6 ASSESSMENT OF LUCIFERASE ACTIVITY AND FLUORESCENCE

- **Cell Lysis**

Lysis buffer was mixed, 50 µl of buffer were added immediately to each well of the frozen plate. The plate was covered with tin foil and shaken for ten minutes to allow complete cell lysis.

- **Luminescence and fluorescence readings**

40 µl of lysate were transferred into a black 96-well plate (optimal for subsequent fluorescence readings) and was shaken once more to evenly fill the well.

Assessment of the luciferase activity was then performed with a TECAN GeniosPro plate reader using autoinjection for the tricine-ATP-buffer and luciferin solution (exact recipe see

under C.3.2). Luminescence signals were recorded from each well. In simultaneously, EGFP-derived fluorescence (to account for potential differences in cell number) was monitored.

The settings for the analysis were

Measurement mode	Fluorescence
Excitation wavelength	485 nm
Emission wavelength	520 nm
Gain	Optimal
Number of reads	1
Integration time	1000 µs
Lag time	0 µs
Mirror selection	Dichroic
Time between move and flash	40 ms

Parameters for fluorescence measurement using Tecan GENios™ Pro.

Measurement mode	Luminescence
Integration time	2000 ms
Attenuation	None
Time between move and integration	50 ms
Well kinetic number	1
Well kinetic interval (minimal)	2020 ms
Injector A/B volume	50 µl
Injector A/B speed	200 µl/s
Injection mode	Standard

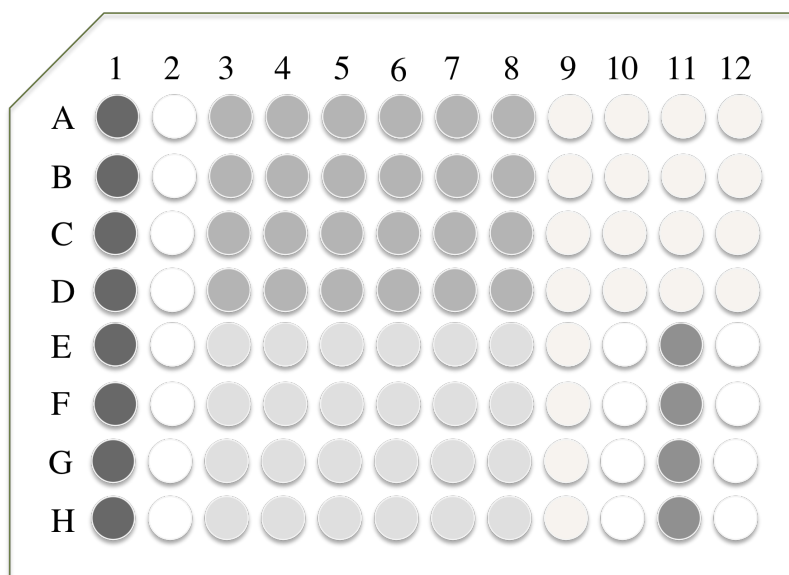**Parameters for luminescence measurement using Tecan GENios™ Pro.**

Figure 9) shows an example of how plates were treated. Wells from A1-H1 were treated with DMSO. Wells from A2-H2 were treated with CDDO-IM. Wells from A3-D8 contained different LC extracts from E3-H8 different PV extracts A9-D12 and E9-H10 with JS extracts, E11-H11 with LS E10-H10 untreated E12-H12 contained just H_2O.

Analysis was done with Excel. The luminescence signal was divided by the fluorescence signal. Then the averages of the single treatments were calculated and divided by the DMSO average. These figures were then transferred to Graph Pad Prism 4.0 to generate a graph.

C.4.0 Quantitative real time PCR (qRT-PCR)

C.4.1 GENERAL

The PCR is a method to replicate specific target regions of a cDNA strand. Therefore it is necessary to exactly know the flanking region so the primer is able to bind. For performing a PCR following substrates are needed: A pair of primers with the flanking sequence of the target, all four desoxyribonucleoside triphosphates (dNTPs) and a heat stable DNA polymerase. Specific primers then bind to cDNA and polymerase is then able to start the translation [49]. One PCR cycle looks like this.: The cDNA is heated to 95°C to denature. Temperature comes down to 54°C (may vary according to the primers). Now the primers can attach to their specific (complementary) region within the template. In the next step temperature rises to 72°C so polymerase is able to bind and start translation

of the region of interest.

These three steps determine one cycle.

In this process qRT-PCR is done, which is slightly different to the PCR method. Additionally a fluorescence dye is used to get a quantifiable signal. This molecule sends a light signal when bound in between the cDNA double strands. After a critical amount of cDNA is reached, the light signal is strong enough to be detected.

This signal gives the Ct (cycle threshold) value, which is important for further calculations. Following graph shows the steps of a qRT-PCR.
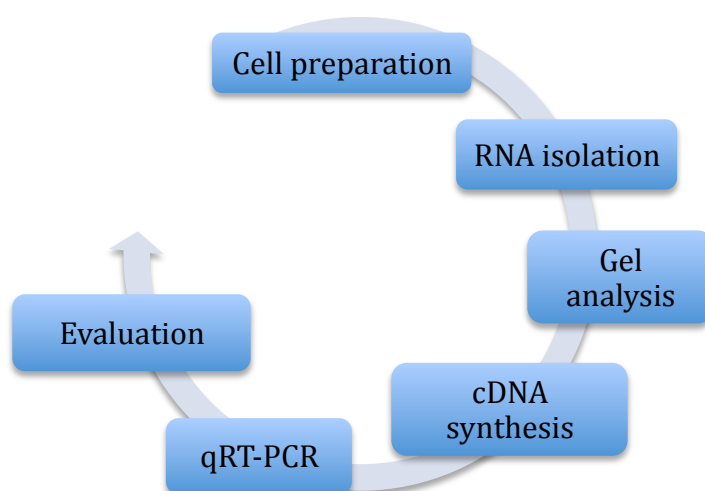
Figure 10) Shows the workflow of qRT-PCR.

C.4.2. MATERIAL

Technical Equipment

Name	Provider
Light Microscope Olympus CKX 31	Olympus Europe GmBH (Hamburg, Germany)
Vi-Cell™ XR Cell Viability Analyzer	Beckman Coulter (Fullerton, CA, USA)
Galaxy Mini Microcentrifuge	Thermo Fisher Scientific Inc.(Waltham, CA, USA)
Vortex Shaker	VWR International Inc. (West Chester, PA, USA)
Dry Block QBD2 2-Bloc system	Grant (Cambridge, UK)
Thermo mixer compact	Eppendorf Austria GmbH (Vienna, Aut)

Light cycler® 480	Roche (Mannheim, Ger.)
UV-Cabinet UVT-S-AR	Biosan (Riga, LV)
Heraeus™Labofuge 400	Thermo Fisher Scif. Inc. (Waltham, CA, USA)
OWL Separation Systems, Inc Model B3	Thermo Fisher Scif. Inc. (Waltham, CA, USA)
OWL Separation Systems, Inc Model B1	Thermo Fisher scif. inc.(Waltham, CA, USA)
Biostep Dunkelhaube	Biostep (Wolferstadt, Ger)
Biostep Transilluminator Bio view UV light	Biostep (Wolferstadt, Ger)

Reagents

peqGold Total RNA Kit

	DNA Removing columns
	Perfect bind- RNA columns
	Collection tubes
	RNA Lysis Buffer T
	RNA Wash Buffer 1
	RNA Wash Buffer 2
	RNase free Water

peqGOLD DNase 1 Digest Kit

| | DNase 1 (RNase free) peqlab 20 U/µl |
| | Digestion buffer for DNase 1 (RNase free) |

qRT-PCR

| | Light cycler® 480 Sybr Green 1 Master H2O, PCR grade |
| | Light cycler® 480 Sybr Green 1 Master 2 x conc. |

TBE Buffer 10 x

Tris	108 g
Boric acid	55 g
0.5 M EDTA pH 8.0	40 ml
Aqua dest.	ad 1000 ml

TBE Buffer 0,5 x

	TBE Buffer 10 x	50 ml
	Aqua dest.	ad 1000 ml

Quick-Load® 100 bp DNA Ladder   **New England Biolabs inc. Ipswich, MA USA**

Loading dye 6 x	peqlab	Erlangen, Ger
RNA Gel 1 %	Agarose	1 g
	TBE 0.5 x	ad 100 g
cDNA Gel 2 %	Agarose	2 g
	TBE 0.5 x	ad 100 g

cDNA transcription

Solution	Producer
0.1 M DTT	Invitrogen
10 mM dNTP mix	Invitrogen
DEPC-treated water	Invitrogen
Random Hexamers	Invitrogen
10 x RT Buffer	Invitrogen
Superscript 2 Reverse Transcriptase 50 μm	Invitrogen
RNaseH E.Coli 10 U/μl	Ambion
Control RNA 50 ng/μl	Invitrogen
RNase Out® Recombinant Ribonuclease inhibitor 5000U (40 U/μl)	

RT-PCR primer

Solution	Producer
HPRT Quanti tect® primer Assay(10 x)	Quiagen
HMox 1 murine Fwd 100 μM	Invitrogen
(sequence AGGTACACATCCAAGCCGAGA)	
HMox 1 murin rev 100 μM	Invitrogen
(sequence: CCATCACCAGCTTAAAGCCTT)	

C.4.3 CELL PREPARATION

MEF WT, MEF Nrf2 KO or MEF AMPK KO cells were used for the analyses. For RNA extraction they were seeded in 6 cm dishes at a concentration of 500.000 cells/dish the day before treatment. Treatment was done with XN (5 μM and 10 μM) and CDDO IM (100 nM) for the indicated periods of time. DMSO (0.1 %) was used as negative control.

As in the other experiments the serum concentration of the used growth medium was reduced from 10 % to 2 % during the incubation with compounds.

C.4.4 RNA ISOLATION

After the desired incubation with test compounds, cells were washed with 10 ml PBS. Then 400 µl RNA lysis buffer was added and left on the cells for 5 minutes at room temperature. To extract the RNA peqGOLD total RNA Kit was used following exactly the manufacturer´s instructions. The kit included the following steps:

a) DNA removal:

Lysed cells were transferred into DNA removing columns. These columns were plugged in collection tubes. After loading them with the lysate, tubes were centrifuged at 12.000 x g for one minute. The removing column was discarded. The flow-through lysate was filled into a new 1.5 ml tube.

b) RNA isolation:

To isolate the RNA the samples were mixed with an equal volume of ethanol 70 %. This solution had to be vortexed and centrifuged, before transferring it to a RNA binding column. The RNA column was then put into a collection tube. Then the next centrifugation step at 10.000 x g for one minute was performed. The RNA binding column, now containing the RNA was used for further steps. The flow-through liquid was discarded.

c) DNA digestion:

To remove every trace of residual DNA, which could interfere with the desired proper analysis of mRNA, an extra DNase digestion step was executed. 75 µl of the pre-mixed DNase digestion mix were added to the membrane of the RNA binding column. Then an incubation for 15 min at room temperature was started. The column was then put into a fresh collection tube and washed and dried according to the protocol of the manufacturer.

d) Elution:

Then the column was put into a clean 1.5 ml reaction tube and filled with 50 µl of sterile RNase free dH$_2$O. The column was centrifuged at a speed of 5.000 x g per minute. The flow through contained the total RNA of the sample and was stored at -80°C for further use or immediately used for additional experiments.

Gel analysis

To see if the extracted RNA was intact and not degraded, a gel run was performed. A 1 % agarose gel in 0.5 x TBE with SybrOrange as nucleic acid dye was prepared. 8 µl of extracted sample were mixed with 2 µl loading buffer, transferred to the gel, and the gel run was done with 150 V for about 90 minutes in 0.5 x TBE buffer. After the run was finished, RNA was viewed under UV light (UV station, biostep), and the gel was photographed (imaging software by Argus). Usually, an intact RNA sample is indicated by two strong bands, representing the 18 S and 28 S ribosomal RNA (optimally in a ratio 1:2). An exemplary photo of a control RNA gel is shown below.
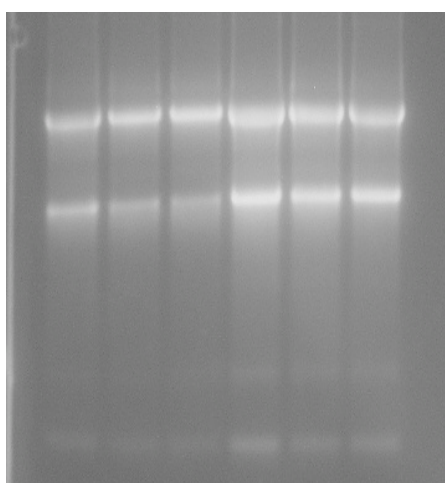
Figure 11) RNA was detected with a 2 % agarose gel mixed with cyberOrange. 8 μl sample was mixed with 2 μl loading buffer. Gel run was performed with 150 V for 90 min. The two visible bonds are 18 and 28 s ribosomal RNA in a relation of 2:1. The first three bonds (from left to right) are MEF Nrf2 WT and the last three MEF Nrf2 KO samples.

C.4.5 CDNA SYNTHESIS

To reverse transcribe the isolated RNA into cDNA, random hexamers were used. A mix of 4 µl sample RNA 1 µl of 10 mM dNTP, 1 µl random hexamers (50 ng/µl), 4 µl DEPC-treated water was used for one sample. To verify the validity of the method two more samples, a positive (RT +, expected to give a signal in the qPCR analysis) and a negative control (RT-, expected to give no signal at all in the qPCR) were prepared with provided control RNA instead of sample RNA.

The reaction mixtures were then incubated at 65°C for 5 minutes and afterwards placed on ice for at least 1 minute.

Next, the master mix for the reverse transcriptase solution was prepared as follows (volumes for one sample, to be up scaled according to the number of samples in one experiment) :

10 x RT buffer	2 µl,
25 mM MgCl$_2$	4 µl,
0,1 M DTT	2 µl,
RNaseOUT™ (40 U/µl)	1 µl.

This RT mix was then added to the samples (mix of RNA, primers and nucleotides), incubated at room temperature for two minutes before 1 µl of SuperScript™2 RT was added, except to the RT-control, which was supplemented with 1 µl water instead of SuperScript™2 RT. Then the samples were incubated for 10 minutes at room temperature, 50 minutes at 42°C, and in order to terminate the reaction at 70°C for 15 min. Then they were chilled on ice. Centrifugation was undertaken to collect potential condensate at the bottom of each tube.

In order to remove RNA from the sample, 1 µl RNase H was added to each tube and incubated for 20 min at 37°C. The ready cDNA samples were stored at -80°C or immediately used for qPCR analysis

C.4.6 QRT-PCR RUN

In order to quantify the cDNA transcript of interest in one sample, a SybrGreen-based qRT-PCR analysis was performed. For this, specific primers, the cDNA of interest (in our case the cDNA for heme oxygenase 1 (HO-1; inducible target gene) or hypoxanthine phosphoribosyltransferase (HPRT, constitutive reference gene)), light cycler 480 SybrGreen mix (Roche) and water were mixed as follows (volumes for one sample, to be up scaled according to the number of samples in one experiment):

Primer mix (fwd + rew; 1 µM)	4 µl,
SybrGreen mix (Roche) (2 x)	7.5 µl,
PCR-graded water	1.5 µl.

A white RT-PCR plate was then loaded with 13 µl of primer/SybrGreen mix and 2 µl of cDNA in triplicate. While pipetting, the RT-PCR plate was placed on ice to keep a constant temperature of 4°C. Moreover, all pipetting steps were done under a (UV) RNA bench. As a negative control 15 µl water in triplicates were added. The latter samples should not give any signal during the entire amplification process.

Finally the plate was sealed with sealing foil, centrifuged and inserted into the RT-PCR machine (Light Cycler, Roche) and the run was started.

qRT-PCR light cycler software 1.5 service pack 4 was used.

The following settings were used for amplification:

95°C	10 min (denaturation)
95°C	5 sec
55°C	5 sec (annealing)
72°C	15 sec (amplification)

50 cycles were performed and SybrGreen-dependent fluorescence was assessed at the end of each amplification cycle. After the run was terminated, a melting curve analysis was added to ensure specific amplification of only one product that should show one distinct melting temperature.

Settings for the melting curve:

95°C	5 sec (denaturation)
60°C	10 sec (melting)
40°C	10 sec (cooling)

For relative quantification of the gene of interest in our samples, we used the $\Delta\Delta Ct$ method. The average Ct values (cycle when fluorescence reached the given threshold) for the target gene (HO-1) and the control gene of each sample (HPRT) were subtracted from each other resulting in a ΔCt value for each sample. The $\Delta\Delta Ct$ value was determined by choosing one calibrator, e.g. WT control cells, to which all other ΔCt values were related by subtraction. The relative change to this calibrator was determined by $2^{-\Delta\Delta Ct}$.

C.5 Flow cytometric analysis of superoxide levels

C.5.1 GENERAL

Flow cytometry is a method used to characterize cells by deviation of light.
A single cell suspension flows through a quartz cuvett which is in front of a laser beam. When a laser ray hits a cell, light is scattered. This signal is measured by two detectors called Forward Side Scatter (FSC) and Side Scatter (SSC). The FSC signal is proportional to the volume of a cell, the light signal in the SSC reflects the granularity of a cell. In addition, fluorescence of special dyes which have been adminstered to the cells, can be excited by the laser and detected. Here Mitosox was used. This dye enters the cell where it is targeted to the mitochondria. As soon as it gets in contact with superoxide, the dye is oxidized and is red fluorescent. The fluorescence signal detected by the FACS machine is therefore a gauge for the cellular load of mitochondrial superoxide.

C.5.2 MATERIAL

Equipment/ConsumablesName	Provider
Heraeus™ Multifuge™ 1 S-R Centrifuge	Thermo Fisher Scientific Inc.(Waltham, CA, USA)
Galaxy Mini Microcentrifuge	Thermo Fisher Scientific Inc.(Waltham,CA,USA)
Vortex Shaker	VWR International Inc. (West Chester, PA, USA)
Eppendorf Pipettes 0.5-10 ml; 1-10 ml; 2-20 ml; 10-1000 ml; 500-5000 ml; multichannel 10-100 ml	Eppendorf Austria GmbH (Vienna, Aut)
Facs Calibur	BD (Franklin Lakes, NY USA)
Facs Flow Supply system	BD (Franklin Lakes, NY USA)
Facs Falcons 5 ml polystyrene round bottom tube	BD (Franklin Lakes, NY USA)

Consumables

Tissue Culture Flask 75 cm^2	Sarstedt GmbH (Nümbrecht, Ger.)
Tissue Culture Dishes (60 mm, 100 mm)	Greiner bio-one (Kremsmünster. Aut)

Reagents

Staining of mitochondria

MitoSOX™ red mitochondrial superoxide indicator 5 µM Invitrogen

Facs Buffer

Solutions	Reagents	
FACS Buffer (for 5 Liters)	NaCl	40.6 g
	KH_2PO_4	1.3 g
	Na_2HPO_4	11.75 g
	KCl	1.4 g
	LiCl	2.15 g
	NaN_3 (Na- Azid)	1.0 g
	Na_2EDTA	1.8 g

Adjust pH to 7.37 and sterile filter it

Solutions	Producer
FACS Clean	BD (Franklin Lakes, NY USA)
FACS Rinse	BD (Franklin Lakes, NY USA)

C.5.3 EXPERIMENTAL PROCEDURE

MEF WT cells were seeded at a concentration of 400.000-500.000 in two kinds of dishes: 6 cm and 10 cm. The dishes were incubated over night.

The next day MitoSox was added to the 10 cm dish in a concentration of 5 µM and left on the cells for 30 min to allow cell entry.

During that time all the treatment solutions and the FACS tubes where prepared and labelled. As positive control Antimycin A (SIGMA), a compound that is known to block complex III of the mitochondrial respiratory chain and thus to trigger mitochondrial superoxide production, was used. Negative control was DMSO.

After 30 minutes, medium (plus residual mitoSOX) was taken off, cells were washed with PBS and trypsinized. 1 ml of mitoSOX-stained cell suspension was filled in each FACS tube and centrifuged for 4 minutes. Supernatant was taken off and the cell pellet was taken up in the respective treatment solutions (0.1 % DMSO, 10 µM Antimycin A or 5-20 µM Xanthohumol in PBS). Fluorescence was assessed immediately in the FL2 channel of the FACS calibur. Before measuring the tube was vortexed and then put into the FACS machine which analyzed 10.000 cells /sample. The development of fluoresence (mean values), indicative for mitochondrial superoxide production, was monitored over 90 to 120 minutes and measured every 15 to 30 minutes. Unstained cells (6-well plate) served as autofluorescence control in the experiment.

C.6 Luciferase-based determination of cellular ATP levels

C.6.1 GENERAL

Luciferase needs ATP to convert luciferin to oxyluciferin which then emits light. In this assay luciferin and a lysis buffer containing luciferase are added to the cells. The higher the cellular content of ATP is, the higher the emitted light which can be read by an appropriate plate reader.
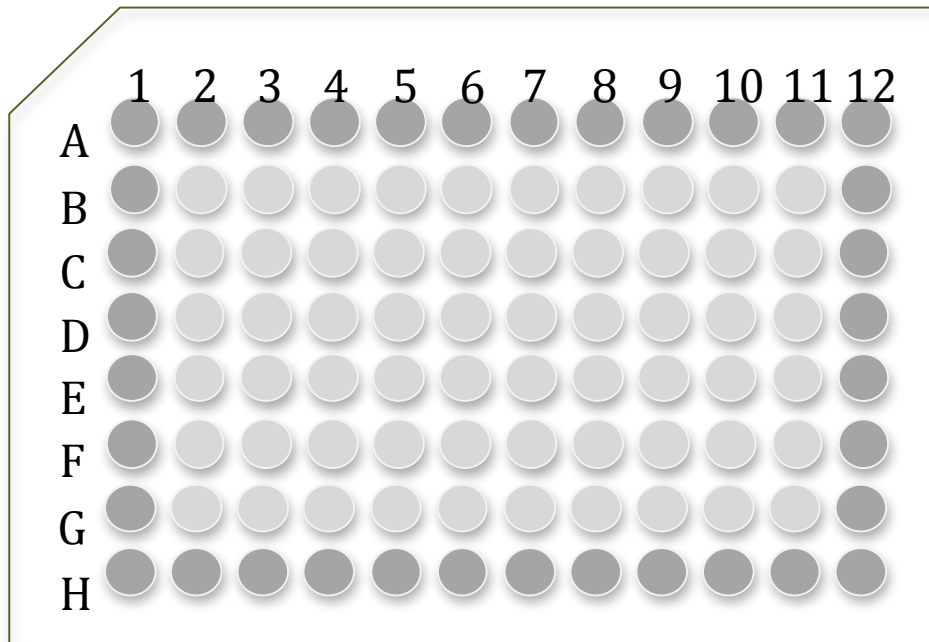
Figure 12) The deep gray wells, containing cells, surrounding the plate are not stimulated. B2-G2 are loaded with DMSO B3-G3 with XN 20 μM B4-G4 with XN 10 μM B5-G5 with XN 5 μM B6-G6 with XN 2,5 μM. This order is repeated from 7-11.

C.6.2 MATERIAL

Devices	Producer
Tecan GENios™Pro, Tecan Sunrise™	Tecan (Mannedorf, Switzerland)
Eppendorf Pipettes	Eppendorf Austria GmbH (Vienna, Aut)
0.5-10 ml; 1-10 ml; 2-20 ml;	
10-1000 ml; 500-5000 ml;	
multichannel 10-100 ml	
Multi-Microplate Genie™	Scientific industries (Bohemia, NY, USA)

Consumables	Producer
96-well Microplates transparent	Greiner bio-one (Kremsmünster, Aut)
96-well Microplates white	Greiner bio-one (Kremsmünster, Aut)

Reagents

CellTiter-glo® Substrate	Promega	(Madison, Wi USA)
CellTiter-glo® Buffer	Promega	(Madison, Wi USA)

C.6.3 EXPERIMENTAL PROCEDURE

MEF cells were seeded into a transluminent 96-well
plate at a concentration of 30.000 per well.
After a day of incubation the test was started. Stimulation
was done with XN in different concentrations (20 µM, 10 µM,
5 µM, 2.5 µM) for 2 hours. As a negative control DMSO
was used. The reaction mix, Cell Titer Glo substrate and Cell
Titer Glo buffer, was prepared ad hoc and pipetted to
the cells according to the manufacturers instructions (Promega).
Lysates were shaken for 10 minutes and
transferred to a white 96-well plate.
Tecan ™Genios Pro was used for luminescence measurement
(integration time 50 ms).

Analysis

Analysis was done with Excel. An average of the
wells filled just with the reaction solution and without cells
was calculated and used as a blank value. This figure was
subtracted from every single well. Then the average value
of each treatment condition was used for creating a graph.
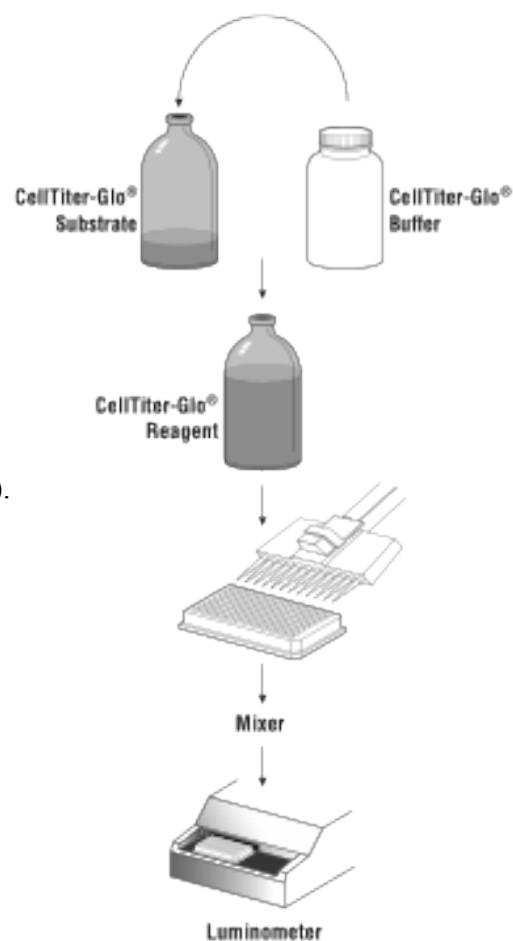
Figure 13) This picture shows the procedure of performing a cell titer glow assay [50].

D) Results

D) Results

D.1 NRF2 ACTIVATION BY THE SELECTED EXTRACTS

Using the ARE-luciferase reporter gene assay, we tested all provided extracts at a concentration of 50 µg/ml for 24 hrs on our CHO-ARE-Luc cells (Figure 14). CDDO-IM at 100 nM served as positive control (known Nrf2 activator).
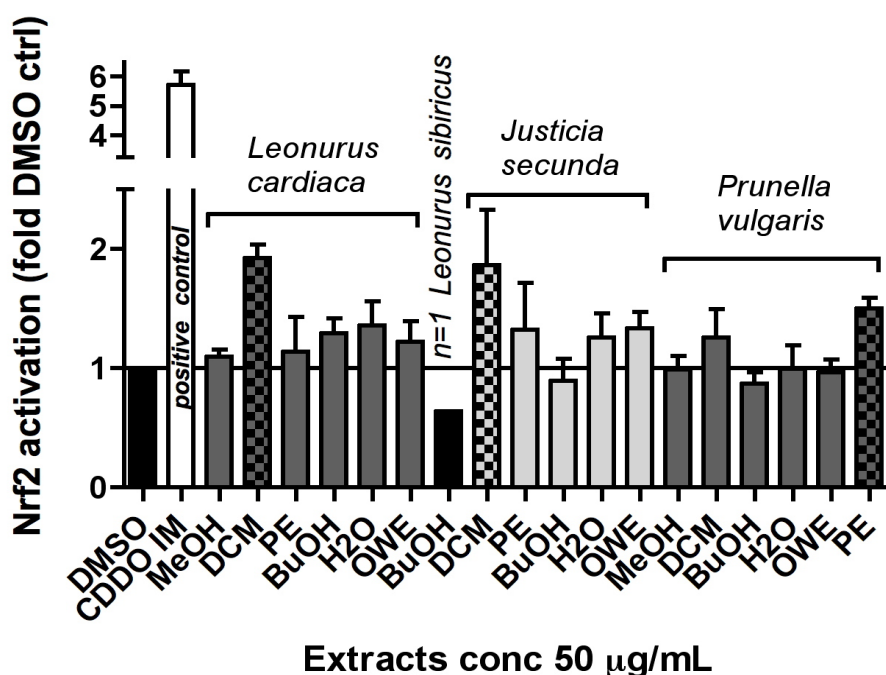
Figure 14) Nrf2 activation by tested extracts after incubation for 24 hours n=3.
CHO-ARE LUC cells were treated with the indicated extracts. Luciferase activity was determined and normalized to fluorescence of EGFP as described in the materials and method part 3.0. Test was repeated three times, and compiled results are shown in the bar graph. All values are expressed as fold Nrf2 activation in comparison to DMSO treated control cells.

As expected, CDDO-IM, the positive control induced Nrf2 activity six times more than DMSO. When looking on the effects of our tested extracts, only some of them induced Nrf2-dependent activation of luciferase expression. The most active extracts were LC DCM, JS DCM and PV PE, inducing a 1.5 to 2 fold activation of Nrf2 at 50 µg/ml. The polar extracts (BuOH, OWE, H_2O) did not show any activating influence on Nrf2.
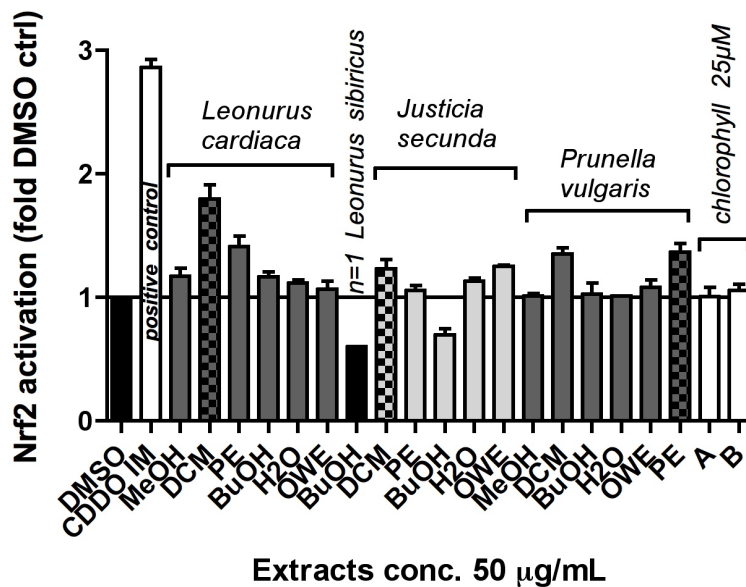
Figure 15) Nrf2 activation by tested extracts after an incubation of 6.5 hrs n=2. 50 μg/ml of the indicated extracts as well as 25 μg/ml chlorophyll A and B (A, B) were administered to CHO-ARE Luc cells for 6.5 hours. Then luciferase activity was assessed and normalized to EGFP fluorescence. Tests were replicated 2 times and compiled results are depicted. All values are expressed as fold Nrf2 activation compared to DMSO treated cells.

Next we wanted to see if the cells react differently when they are stimulated for a shorter period of time. Previous experiments have shown that different compounds show different kinetics in Nrf2 activation with some of them only evoking a transient response between 3 and 8 hours upon treatment. The next tests were therefore performed in the same way as the one before, but instead of incubating with the extracts for 24 hours we now chose a treatment for 6.5 hours (Figure 15). Besides the extracts we also tested chlorophyll A and B (25 µg/ml each) in order to assess its potential to activate Nrf2.

Here we can also see a marked activation of Nrf2 when cells were stimulated with CDDO-IM as positive control (100 nM). The difference to the test before is that the luciferase expression is just 3 times higher than the DMSO value, even though the concentration of CDDO-IM was the same in both settings. This effect is likely to be caused by the reduced time of incubation. With regard to the tested extracts, LC DCM was the most promising Nrf2 activator. JS DCM and PC PE showed a rather moderate activation of Nrf2. These findings are consistent to the results obtained with 24 hrs incubation. Moreover, also the DCM extract of PV elicited Nrf2 activation in this "short time" setting.

When looking at the effect of chlorophyll we can conclude that chlorophylls are not potent activators of Nrf2, and moreover that the activity of the lipophilic test extracts is not solely due to their content of chlorophyll.

In a next step, we investigated the dose-dependency of the identified Nrf2-activating extracts.

We picked LC PE, PV PE, LC DCM, JS DCM, JS BuOH as well as Chloro A Chloro B. Plant extracts were used in a concentration of 25/50/100 µg/ml whereas Chloro A and B in 12.5/25/50 µg/ml.

The incubation time was again 24 hours. Extracts were applied in quadruplets.
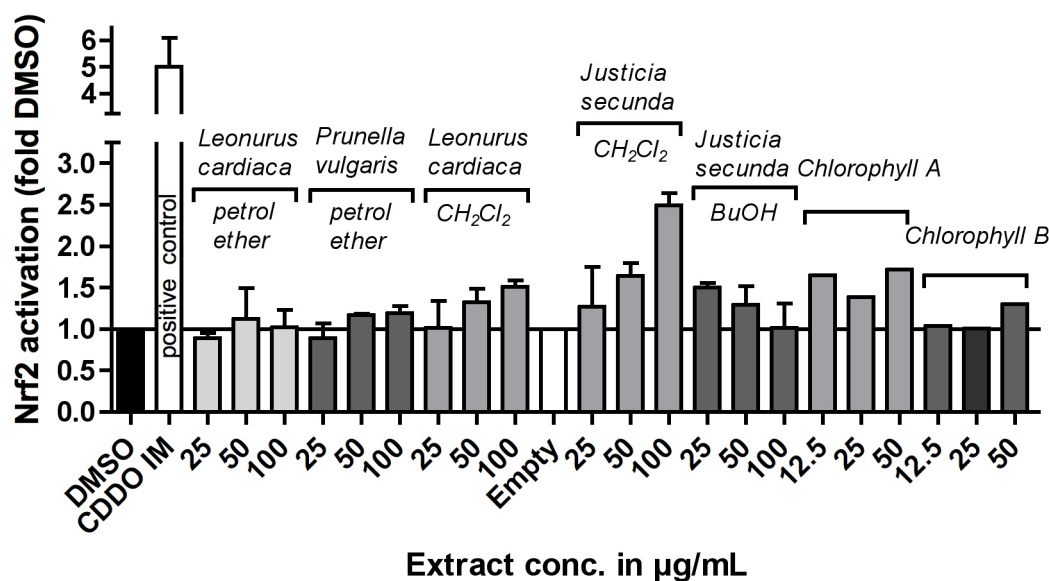

Figure 16) Dose dependent activation of Nrf2 by selected extracts. CHO-ARE Luc cells were incubated with the extracts as indicated for 24 hrs. Then luciferase activity was determined and normalized to EGFP fluorescence. Data are presented as fold DMSO control and are means of 2 experiments with consistent results.

Fig 16 shows the effect on Nrf2 activation of the extracts in different concentrations. CDDO-IM (100 nM) served again as positive control and induced Nrf2-dependent luciferase activity 5-6 fold. The Nrf2 activation by most of the extracts was moderate and lower than in previous experiments. An explanation could be that the active principle in the complex mixture of the extract is unstable in solution, light or temperature sensitive and therefore prone to degradation when thawed or exposed to light. However, we still could see a dose-dependent activation of Nrf2 in the case of LC DCM and JS DCM. JS DCM was the most active extract in this setting and activated Nrf2 almost 3-fold at a concentration of 100 µg/ml. For JS BuOH we even observed an inhibitory action on Nrf2 with increasing concentration. Chlorophyll A and B did not elicit a concentration-dependent activation of Nrf2.

D.1.1 SUMMARY AND OUTLOOK

In summary, we tested 18 extracts for Nrf2 activation in CHO-ARE-Luc cells. From those, four positively influenced Nrf2 activation in our test system. The most active extracts were hereby the DCM extracts of LC and JS. The active principle in these extracts is not, or at least not to a

major extent, chlorophyll, since we observed that chlorophyll does not have a big influence on Nrf2 activation on its own.

Compared to the positive control used, CDDO-IM, the tested extracts appeared as rather weak activators of Nrf2 (maximal 3 fold activation of Nrf2 by JS DCM at 100 µg/ml versus 6-8 fold activation at 100 nM CDDO-IM). However, it is important to note that extracts from plants usually contain a multitude of substances, which may in sum influence each other in a negative way, either by simple dilution of the active principle or by actively antagonizing its action. Like this, it is possible that the active principle is present in just very small amounts and hereby masked by the other components in the extract, or that it is tightly bound to other compounds and thus hardly available for the cell and Nrf2 activation. Depending on the complexity of the individual extracts, removal of chlorophyll and another round of fractionation may already result in more promising results with respect to Nrf2 activation and make it easier to finally decide whether the DCM extracts of JS and LC are good sources for the discovery of (novel) potent Nrf2 activators and worth further bioguided fractionation efforts.

D.2 AMPK/NRF2 Crosstalk

In the second part of this project we focussed on the potential crosstalk between Nrf2 and AMPK. As outlined in the beginning of this thesis, AMPK and Nrf2 share different activities. Both are involved in the cellular protection against redox stress and inflammation and are connected with an improved lipid profile, just to name a few similarities. To elucidate whether both proteins belong to a common signaling network and crosstalk with each other we investigated whether and how the XN-triggered and Nrf2-mediated HO-1 expression is enhanced by AMPK.

D.2.1 CONFIRMATION OF PREVIOUS RESULTS

Previous results showed that XN induces the expression of HO-1 in WT mouse embronic fibroblasts in a period of 16-24 hours, whilst Nrf2 ko cells do not and AMPK ko cells do to a markedly reduced extent. These data suggest that HO-1 expression upon XN exposure is strictly Nrf2-dependent and positively influenced by AMPK.

One of the first aims was to reproduce these findings. Therefore Western Blot experiments were done. XN (5 µM), CDDO-IM (100 nM) and DMSO (0,1 %) were tested on MEF WT, Nrf2 ko and AMPK ko cells.
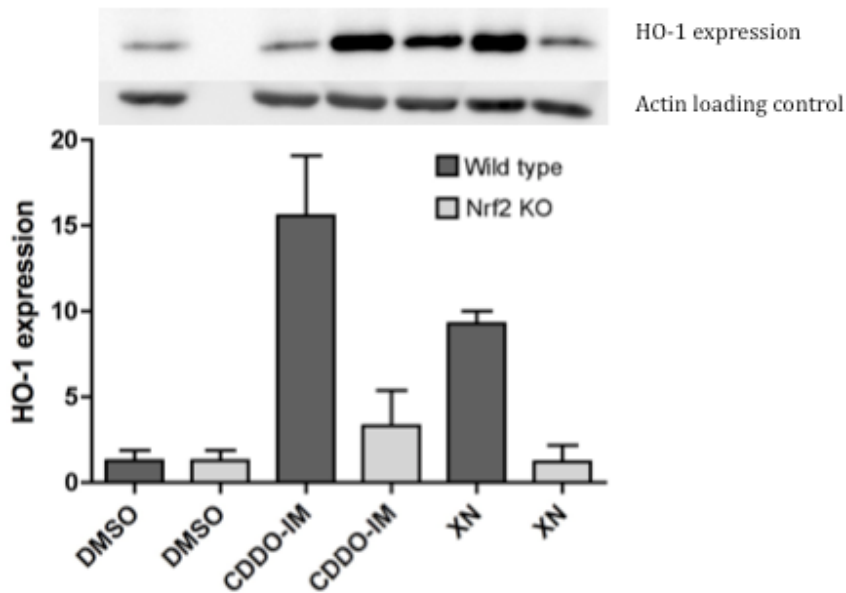
Figure 17) This graph shows Nrf2-dependent HO-1 expression. MEF WT and MEF Nrf2 ko cells where incubated with DMSO (0.1 %) CDDO-IM (100 nM) and XN (5 µM) over a period of 24 hours. HO-1 as an indicator for Nrf2 activation and Actin as loading control were used. n=2

Figure 17 shows that CDDO IM and XN up-regulate HO-1 levels in MEF WT wheras in Nrf2 ko cells no (for XN) or a drastically reduced (for CDDO-IM) effect is seen.

Thus, the Nrf2 dependency of HO-1 induction by CDDO-IM and XN could be successfully confirmed.

Next we examined DMSO, CDDO-IM and XN on MEF WT & AMPK ko for their potential to elevate HO-1 protein expression.
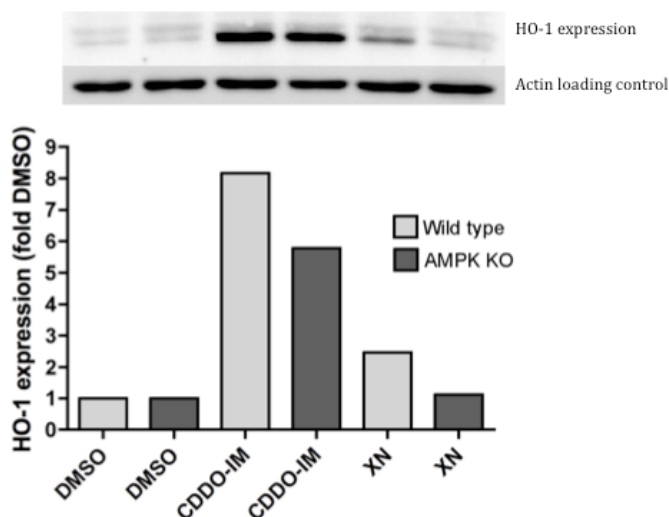
Figure 18) This graph shows that HO-1 expression is AMPK-dependent. MEF WT and MEF AMPK ko cells were incubated with DMSO (0,1 %), CDDO-IM (100 nM) and XN (5 µM) over a period of 24 hours. HO-1 as an indicator of Nrf2 activation and Actin as loading control were used.

As seen in figure 18 CDDO-IM and also XN induce HO-1 expression in WT while the induction in AMPK ko is obvious but smaller than in the WT counterparts. Thus, also the boosting effect of AMPK on HO-1 induction by XN (and CDDO-IM) could be confirmed.

D.2.2 KINETICS OF HO-1 INDUCTION BY XN IN THE DIFFERENT USED CELL TYPES

As the preceding experiments were only performed with one incubation time, we decided to examine the kinetic of HO-1 induction by XN in WT and knockout cells. Such studies could reveal potential differences in the time frame of HO-1 induction upon XN exposure.
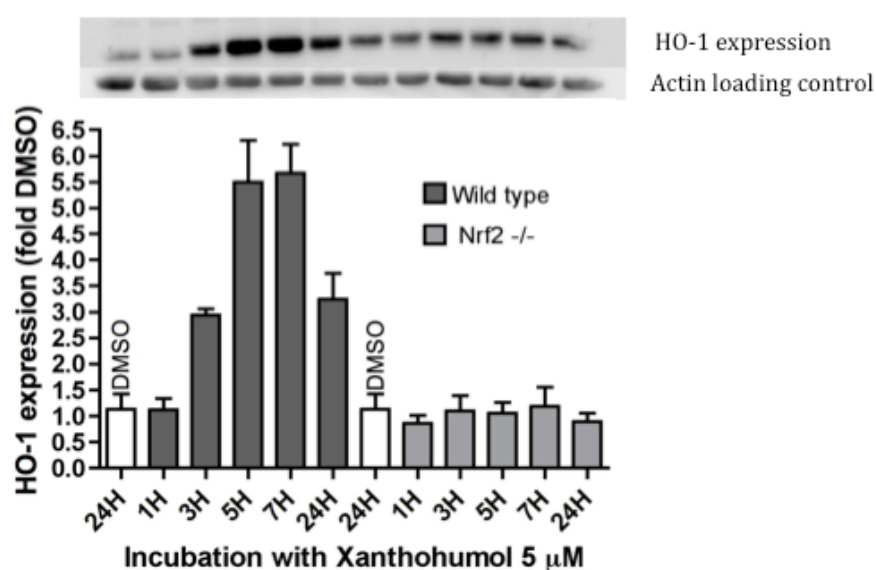
Figure 19) HO-1 expression is time- and Nrf2-dependent. MEF WT and MEF Nrf2 ko cells were incubated with DMSO (0.1 %) and XN (5 µM) over a period of 24 hours. HO-1 as an indicator for Nrf2 activation and Actin as loading control were used. n=2

Figure 19 shows that in WT cells XN induces a maximum of HO-1 levels between 5-7 hours of incubation time, while the 24 hour value of HO-1 levels is still 3 times higher than the DMSO negative control. Nrf2 deficient cells do not respond to a XN incubation with increased HO-1 expression, once more confirming Nrf2-dependency.
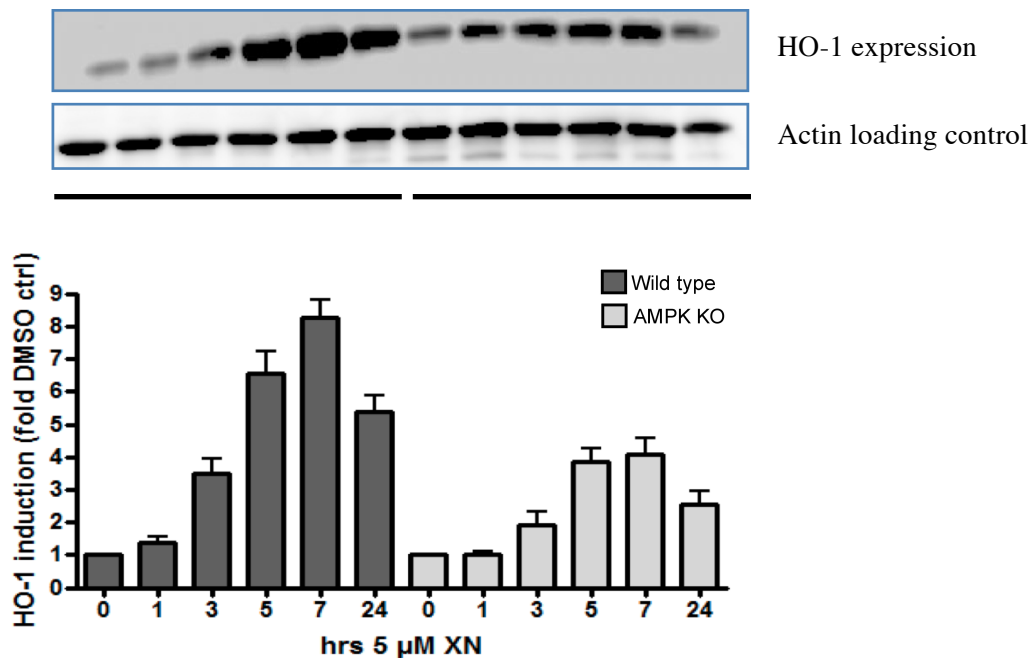
Figure 20) HO-1 expression is time- and AMPK- dependent. Tests where done with XN 5 μM cell preparation already described in materials and methods 1.0-1.3. Western blotting was performed as described in materials and methods 2.0-2.6. n=2

Also, in WT AMPK cells Xanthohumol induced HO-1 maximally between 5-7 hours (Figure 20). In AMPK ko counterparts maximal HO-1 induction is also obtained by XN after 5-7 hrs. However, the maximal induction in AMPK ko cells is less than in WT cells.

These data so far indicate and confirm previous findings, that XN induces HO-1 in MEFs with a maximum after 7 hours of treatment in a strictly Nrf2-dependent manner and that presence of AMPK strongly enhances this activity.

D.2.3. CROSSTALK BETWEEN AMPK AND NRF2

D.2.3.1 GENERAL POSSIBILITIES FOR A COOPERATION BETWEEN AMPK AND NRF2

Generally, there are different possibilities how to explain that AMPK and Nrf2 positively affect HO-1 expression by XN.

First, AMPK and Nrf2 are in a linear dependency, meaning that activation of AMPK is a direct and obligatory upstream mediator of Nrf2 signalling and HO-1 induction.
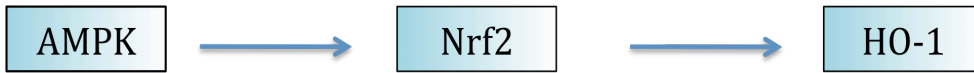
Second, AMPK and Nrf2 could act independently and just additively induce HO-1 levels.
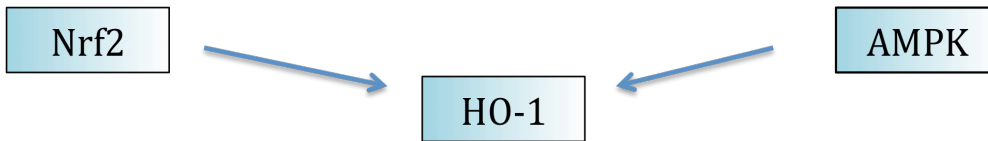
And third, AMPK activation could boost the Nrf2 signal cascade.

D.2.3.2 AMPK/NRF2 CROSSTALK IN XN-TREATED MEFS

Possibility 1)

can be excluded as sole explanation for our observations since we see some HO-1 expression in AMPK ko cells by XN. A strictly linear and obligatory signal flow from AMPK to Nrf2 activation in XN-treated cells can therefore be ruled out.

Nonetheless and intrigued by reports that AMPK activators lead to Nrf2 activation in different cell systems [51], we investigated whether AMPK activation can suffice to induce Nrf2-dependent HO-1 expression in our cells.

We used AICAR, a selective and well known AMPK activator (500 µM), as a stimulating substance in WT and Nrf2 ko as well as in AMPK ko cells. Protein expression of HO-1 was detected by Western Blotting.
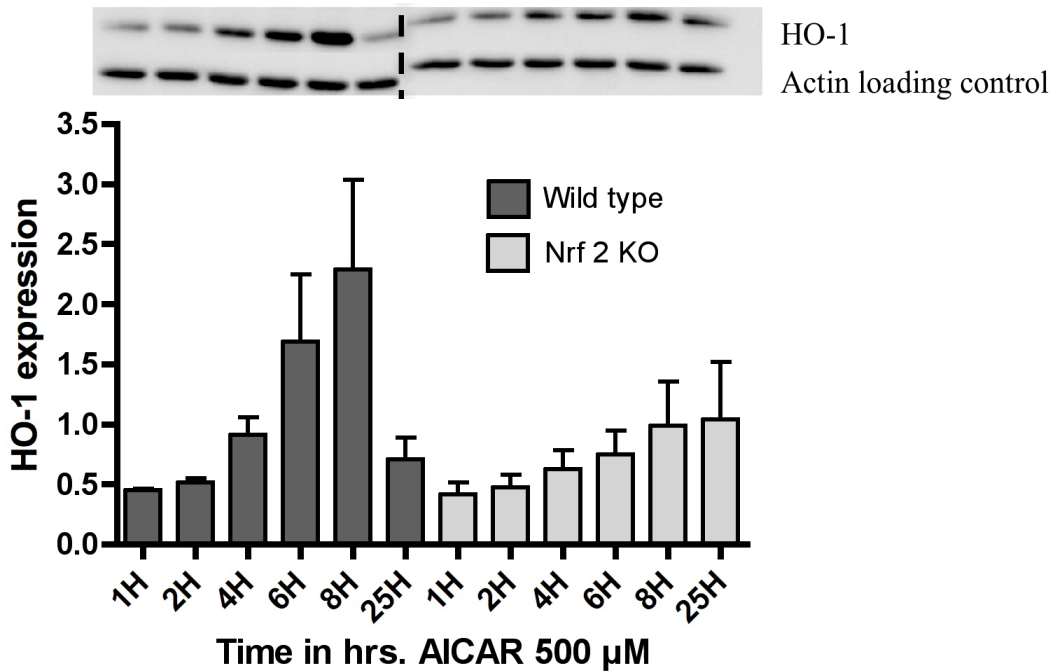
Figure 21) HO-1 expression in response to AICAR (500 μM) is time- and Nrf2-dependent. Cell preparation is described in methods and materials 1.0-1.3. Western Blotting was performed as described in materials and methods 2.0-2.6 n=3

Figure 21 shows that AICAR can induce HO-1 in WT cells and Nrf2 ko cells in a time-dependent manner. The Nrf2 knockout cells, however, show reduced HO-1 induction. These findings suggest that activation of AMPK can induce HO-1 in a partly Nrf2-dependent manner. Next we assessed HO-1 induction by AICAR in WT and AMPK ko cells. As seen in figure 22, AICAR markedly induces HO-1 in WT, but not in AMPK ko cells. This finding indicates that AICAR induces HO-1 in MEFs in a strictly AMPK-dependent manner.
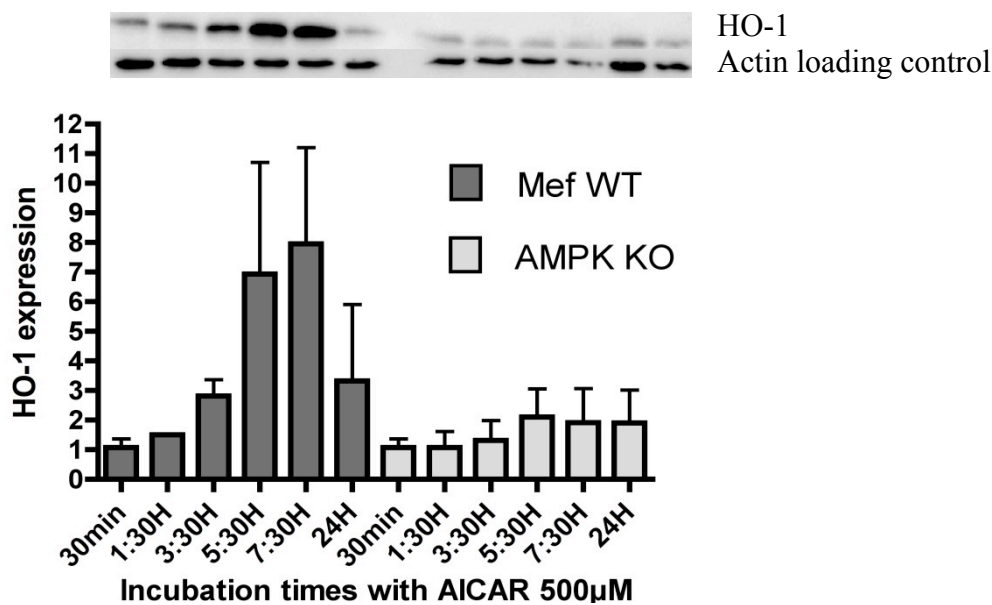
HO-1
Actin loading control

Figure 22) HO-1 expression in response to AICAR is time- and AMPK-dependent. Cell preperation is described in methods and materials 1.0-1.3. Western Blotting was performed as described in materials and methods 2.0-2.6 n=3

Overall we can conclude that AICAR activates AMPK and that AMPK activation is crucial for HO-1 induction by AICAR. Nrf2 seems to be one, but not the only transcription factor involved in HO-1 induction by AICAR and AMPK activation. The existence of a direct and linear signaling axis from AMPK activation to Nrf2 activation cannot generally be excluded by these findings.

The second possibility of crosstalk with regard to HO-1 induction by XN is the additive action of AMPK and Nrf2. This would mean that XN activates AMPK and Nrf2 independently from each other and the net induction of HO-1 is merely the sum of AMPK and Nrf2 action. However, looking at the Western Blot data we could rule out this possibilty since there was no HO-1 induction at all in Nrf2 knockout cells.

As Western Blot in general is not very sensitive and only semiquantitative we aimed to confirm these data by quantitative RT-PCR, a method which is also usefull for investigating possibility 3.

For this we first had to optimize conditions for amplification of HO-1. As seen in figure 23, after optimization of primer sequence, selected amplicon and annealing temperature we managed to specifically amplify one product only (right panel). This constituted a major improvement to the initial pilot experiments (left panel) where we could see bands of three different sizes as putative specific HO-1 amplification products.
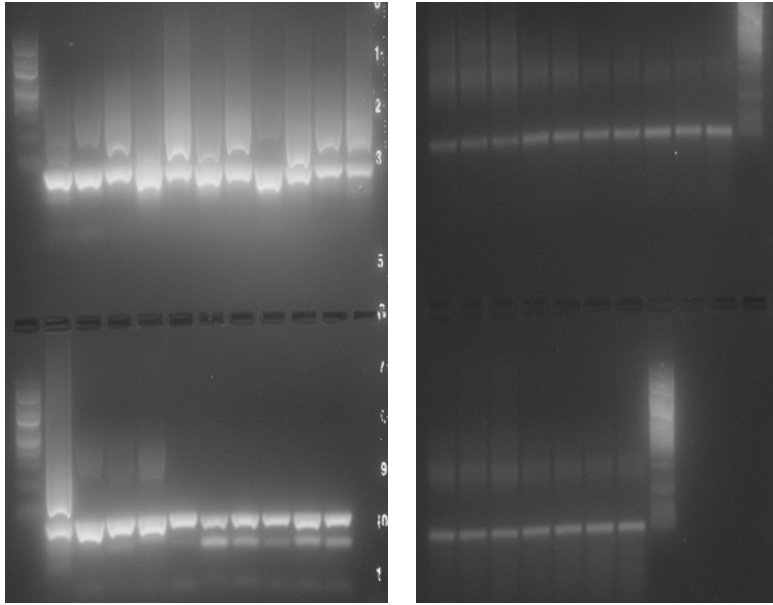
Figure 23) The picture on the left shows the first attempt of RT-PCR. The very left band is a standard and the following bands are duplicates of cDNA that should show just one band. Here we find a multitude of bands, telling us that the products are not focusing on one single cDNA strand. The picture on the right shows the optimized procedure. The standard is on the right. Here we can see a consistent cDNA product in every band. A second band is still present, which we could not reduce after multiple tests.

With this method at hand, we then wanted to find the incubation time which is best to check for HO-1 mRNA levels after Nrf2 activation. For this, we used CDDO-IM (100 nM) as positive control. As figure 24 shows, mRNA levels of HO-1 reached a marked upregulation after 4 hrs incubation.
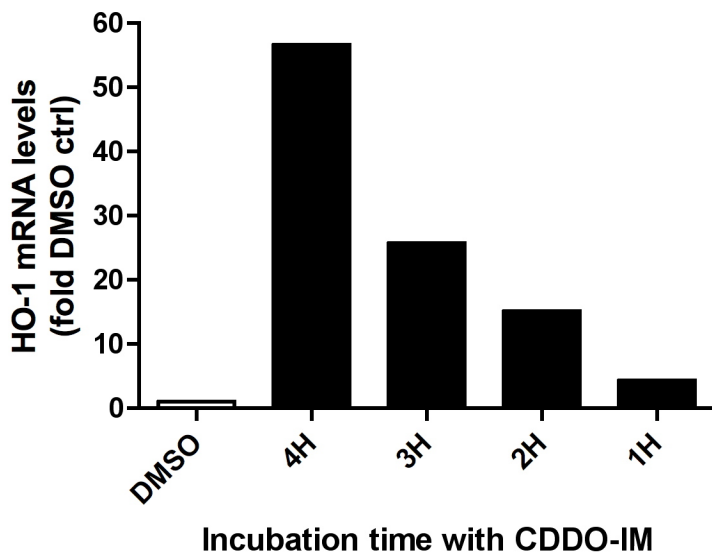

Figure 24) HO-1 levels in WT cells after incubation with CDDO-IM (100 nM) at a period of overall 4 hours. qRT-PCR was performed HPRT served as endogenous control.

After this optimization process we checked HO-1 mRNA levels after XN exposure in WT, Nrf2 ko and AMPK ko cells.

In figure 25, one can observe massive induction of HO-1 in WT cells by XN, but no induction in Nrf2 ko cells. These data are in line with the Western Blot data and confirm our finding that the indution of HO-1 by XN is Nrf2 dependent and cannot be achieved by AMPK activation alone. The increased HO-1 expression in AMPK WT compared to AMPK ko cells cannot be explained by the additive action of Nrf2 and AMPK on the HO-1 promoter.
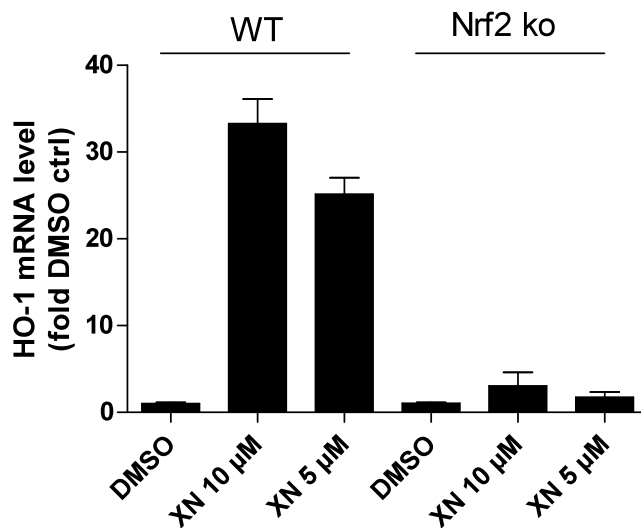

Figure 25) qRT-PCR was performed showing mRNA levels of HO-1 after dose-dependent incubation with Xanthohumol on MEF WT and Nrf2 ko cells for 4 hrs. n=3

In figure 26, we can see that XN concentration dependently induces HO-1 mRNA levels both in WT and AMPK ko cells. The extent in ko cells is, however, lower than in WT cells. These data are in concordance with our previous Western Blot data and go inline with possibility three: AMPK boosts the strictly Nrf2 dependent HO-1 transcription by XN.
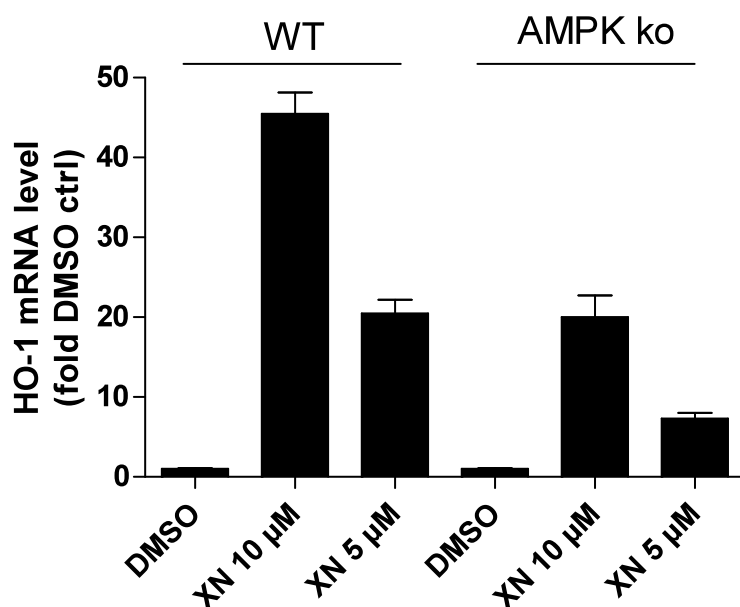
Figure 26) qRT-PCR was performed showing mRNA levels of HO-1 in MEF WT and AMOK ko cells incubated with Xanthohumol at different concentrations for 4 hrs. n=3

From all these data we can conclude:

➔ HO-1 induction by XN is strictly dependent on Nrf2 in MEF
➔ The presence of AMPK boosts Nrf2-dependent HO-1 induction by XN
➔ AMPK enhances Nrf2 activity already at the level of transcription.

How AMPK positively influences Nrf2 activity needs to be investigated in future studies which should focus in detail on the complex molecular crosstalk between Nrf2 and AMPK.

D.2.4 ACTIVATION OF AMPK BY XN

In this thesis we further adressed the question how XN may obtain AMPK activation which apparently underlies the increased HO-1 induction in WT over AMPK ko cells.

In a first attempt we investigated potential changes in AMPK phosphorylation (at Thr 172) by treatment with different concentrations of XN for different periods of time. However, we were not able to observe a reproducible pattern which would allow reliable conclusions (data not shown).

As AMPK is activated by an elevated AMP/ATP ratio, we also tried to assess cellular ATP levels upon XN exposure. For this, we used a luminescence-based method for ATP detection and treated cells for different periods of time and with different concentrations of XN. As seen

in figures 27 and 28, XN did not cause obvious time-or concentration-dependent changes in the cellular ATP levels. However, at this point it should be noted that this method is not very sensitive in order to assess alterations in the AMP/ATP ratio. A more sensitive approach would be to determine both cellular AMP and ATP levels by HPLC .
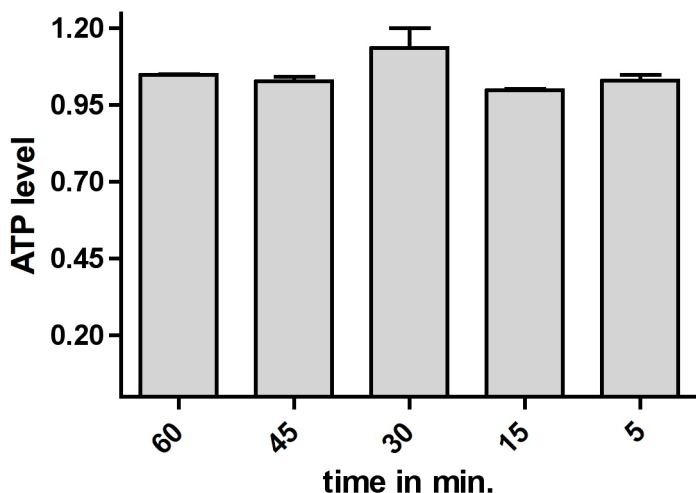

Figure 27) ATP levels of MEF after incubation with XN 5 μM for the indicated periods of time.
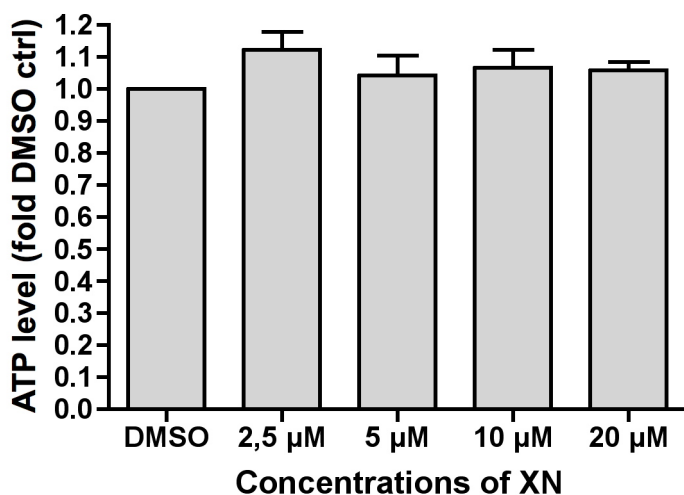

Figure 28) ATP levels in MEF treated with XN at different concentrations for 60 min.

As an impaired electron transport can cause reduced ATP production in the oxidative phosphorylation, and XN has been reported to cause enhanced mitochondrial superoxide production in cancer cells [52], we were curious whether this may also be true for our cell system and our used concentration of XN. For determination of mitochondrial superoxide we used Mitosox®, a dye that selectively binds to mitochondria and, if it is oxidized, sends out a fluorescence signal.

As positive control antimycin A in a concentration of 10 μM was used. This compound interacts with complex III of the oxidative phosphorylation, leading to a stop in the protein-mediated electron transfer chain and to a direct reduction of oxygen to superoxide. In figure 29

we monitored mitochondrial superoxide levels over a period of 90 min after treatment. XN was tested in three different concentrations. DMSO served as a negative control while antimycin was the positive control. Cells (DMSO- ; XN-) without mitoSOX served as autofluorescence control. In DMSO-treated cells, mitoSOX fluorescence and thus mitocondrial superoxide production only marginally increases over time. XN, however, leads to a dose- and time-dependent increase of mitochondrial superoxide production which is also at 5 µM higher than in the DMSO control cells. 20 µM XN even leads to a higher superoxide production than antimycin.
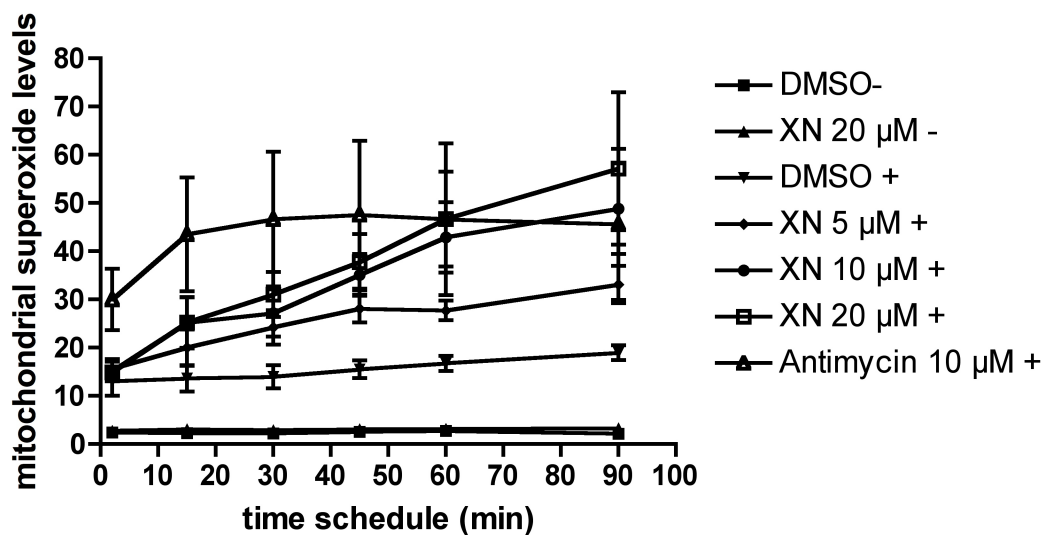

Figure 29) Superoxide levels induced by XN (5 μM, 10 μM, 20 μM), Antimycin and DMSO, over a period of 90 minutes. n=3.

These data demonstrate that XN leads to an increased mitochondrial superoxide production. This may mean that the mitochondrial electron transport chain is impared by XN which in turn could lead to reduced ATP production by OXPHOS and finally AMPK activation. This hypothesis needs to be tested in future studies e.g. on isolated mitochondria or sophisticated assays checking mitochondrial functionality in cells or with sensitive detection of AMP and ATP levels.

D.2.5 Summary and outlook

Overall, we could reveal that there is crosstalk between AMPK and Nrf2 during the induction of HO-1 expression by XN. Cells lacking AMPK express less HO-1 as WT cells. This phenomenon is obvious on the protein- and mRNA level, suggesting a positive effect of AMPK on an event prior to / during transcription or on mRNA stability of HO-1. Details must be investigated in future studies which could include examination of nuclear levels of Nrf2 or the phosphorylation status of Nrf2 in WT and AMPK ko cells after XN exposure. How XN may

activate AMPK also requires further attention. Although we were able to observe increased mitochondrial superoxide production, indicative for an impaired electron transport, we could not detect major changes in ATP levels or consistent changes of AMPK phosphorylation in XN-treated cells.

E) References

E) References

1.   Kensler, T.W., N. Wakabayashi, and S. Biswal, Cell survival responses to environmental stresses via the Keap1-Nrf2-ARE pathway. Annu Rev Pharmacol Toxicol, 2007. 47: p. 89-116.

2.   Tong, K.I., et al., Keap1 recruits Neh2 through binding to ETGE and DLG motifs: characterization of the two-site molecular recognition model. Mol Cell Biol, 2006. 26(8): p. 2887-900.

3.   Tong, K.I., et al., Two-site substrate recognition model for the Keap1-Nrf2 system: a hinge and latch mechanism. Biol Chem, 2006. 387(10-11): p. 1311-20.

4.   Sekhar, K.R., G. Rachakonda, and M.L. Freeman, Cysteine-based regulation of the CUL3 adaptor protein Keap1. Toxicol Appl Pharmacol, 2010. 244(1): p. 21-6.

5.   Katoh, Y., et al., Evolutionary conserved N-terminal domain of Nrf2 is essential for the Keap1-mediated degradation of the protein by proteasome. Arch Biochem Biophys, 2005. 433(2): p. 342-50.

6.   Li, L., et al., Molecular evolution of Keap1. Two Keap1 molecules with distinctive intervening region structures are conserved among fish. J Biol Chem, 2008. 283(6): p. 3248-55.

7.   van Muiswinkel, F.L. and H.B. Kuiperij, The Nrf2-ARE Signalling pathway: promising drug target to combat oxidative stress in neurodegenerative disorders. Curr Drug Targets CNS Neurol Disord, 2005. 4(3): p. 267-81.

8.   Ruotsalainen, A.K., et al., The absence of macrophage Nrf2 promotes early atherogenesis. Cardiovasc Res, 2013. 98(1): p. 107-15.

9.   Yagishita, Y., et al., Nrf2 Protects Pancreatic beta-Cells from Oxidative and Nitrosative Stress in Diabetic Model Mice. Diabetes, 2013.

10.   Furukawa, S., et al., Increased oxidative stress in obesity and its impact on metabolic syndrome. J Clin Invest, 2004. 114(12): p. 1752-61.

11.   Kensler, T.W. and N. Wakabayashi, Nrf2: friend or foe for chemoprevention? Carcinogenesis, 2010. 31(1): p. 90-9.

12.   Jaramillo, M.C. and D.D. Zhang, The emerging role of the Nrf2-Keap1 signaling pathway in cancer. Genes Dev, 2013. 27(20): p. 2179-91.

13.   Shibata, T., et al., Genetic alteration of Keap1 confers constitutive Nrf2 activation and resistance to chemotherapy in gallbladder cancer. Gastroenterology, 2008. 135(4): p. 1358-1368, 1368 e1-4.

14.   Mitsuishi, Y., H. Motohashi, and M. Yamamoto, The Keap1-Nrf2 system in cancers: stress response and anabolic metabolism. Front Oncol, 2012. 2: p. 200.

15.   Foresti, R., et al., Small molecule activators of the Nrf2-HO-1 antioxidant axis modulate heme metabolism and inflammation in BV2 microglia cells. Pharmacol Res, 2013. 76: p. 132-48.

16.   Salt, I., et al., AMP-activated protein kinase: greater AMP dependence, and preferential nuclear localization, of complexes containing the alpha2 isoform. Biochem J, 1998. 334 (Pt 1): p. 177-87.

17.   Suter, M., et al., Dissecting the role of 5'-AMP for allosteric stimulation, activation, and deactivation of AMP-activated protein kinase. J Biol Chem, 2006. 281(43): p. 32207-16.

18.   Hawley, S.A., et al., Characterization of the AMP-activated protein kinase kinase from rat liver and identification of threonine 172 as the major site at which it phosphorylates AMP-activated protein kinase. J Biol Chem, 1996. 271(44): p. 27879-87.

19.   Xiao, B., et al., Structure of mammalian AMPK and its regulation by ADP. Nature, 2011. 472(7342): p. 230-3.

20.   Hawley, S.A., et al., 5'-AMP activates the AMP-activated protein kinase cascade, and Ca2+/calmodulin activates the calmodulin-dependent protein kinase I cascade, via three independent mechanisms. J Biol Chem, 1995. 270(45): p. 27186-91.

21.   Hardie, D.G., F.A. Ross, and S.A. Hawley, AMPK: a nutrient and energy sensor that maintains energy homeostasis. Nat Rev Mol Cell Biol, 2012. 13(4): p. 251-62.

22.   Hardie, D.G., AMP-activated/SNF1 protein kinases: conserved guardians of cellular energy. Nat Rev Mol Cell Biol, 2007. 8(10): p. 774-85.

23.   Sakamoto, K. and G.D. Holman, Emerging role for AS160/TBC1D4 and TBC1D1 in the regulation of GLUT4 traffic. Am J Physiol Endocrinol Metab, 2008. 295(1): p. E29-37.

24.   Muoio, D.M., et al., AMP-activated kinase reciprocally regulates triacylglycerol synthesis and fatty acid oxidation in liver and muscle: evidence that sn-glycerol-3-phosphate acyltransferase is a novel target. Biochem J, 1999. 338 (Pt 3): p. 783-91.

25.   Clarke, P.R. and D.G. Hardie, Regulation of HMG-CoA reductase: identification of the site phosphorylated by the AMP-activated protein kinase in vitro and in intact rat liver. EMBO J, 1990. 9(8): p. 2439-46.

26.   Jorgensen, S.B., et al., The alpha2-5'AMP-activated protein kinase is a site 2 glycogen synthase kinase in skeletal muscle and is responsive to glucose loading. Diabetes, 2004. 53(12): p. 3074-81.

27.   Winder, W.W., et al., Activation of AMP-activated protein kinase increases mitochondrial enzymes in skeletal muscle. J Appl Physiol (1985), 2000. 88(6): p. 2219-26.

28.   Thomas, A., et al., Quantification of AICAR-ribotide concentrations in red blood cells by means of LC-MS/MS. Anal Bioanal Chem, 2013.

29.   Kroller-Schon, S., et al., alpha1AMP-activated protein kinase mediates vascular protective effects of exercise. Arterioscler Thromb Vasc Biol, 2012. 32(7): p. 1632-41.

30.   Carling, D., et al., AMP-activated protein kinase: new regulation, new roles? Biochem J, 2012. 445(1): p. 11-27.

31.   Hardie, D.G., Role of AMP-activated protein kinase in the metabolic syndrome and in heart disease. FEBS Lett, 2008. 582(1): p. 81-9.

32.   Hawley, S.A., et al., Use of cells expressing gamma subunit variants to identify diverse mechanisms of AMPK activation. Cell Metab, 2010. 11(6): p. 554-65.

33.   Gerhauser, C., et al., Cancer chemopreventive activity of Xanthohumol, a natural product derived from hop. Mol Cancer Ther, 2002. 1(11): p. 959-69.

34.   Tronina, T., et al., Antioxidant and antiproliferative activity of glycosides obtained by biotransformation of xanthohumol. Bioorg Med Chem Lett, 2013. 23(7): p. 1957-60.

35.   Dorn, C., et al., Xanthohumol, a chalcon derived from hops, inhibits hepatic inflammation and fibrosis. Mol Nutr Food Res, 2010. 54 Suppl 2: p. S205-13.

36.   Blanquer-Rossello, M.M., et al., Effect of xanthohumol and 8-prenylnaringenin on MCF-7 breast cancer cells oxidative stress and mitochondrial complexes expression. J Cell Biochem, 2013. 114(12): p. 2785-94.

37.   Kim, S.Y., I.S. Lee, and A. Moon, 2-Hydroxychalcone and xanthohumol inhibit invasion of triple negative breast cancer cells. Chem Biol Interact, 2013. 203(3): p. 565-72.

38.   Gerhauser, C., Broad spectrum anti-infective potential of xanthohumol from hop (Humulus lupulus L.) in comparison with activities of other hop constituents and xanthohumol metabolites. Mol Nutr Food Res, 2005. 49(9): p. 827-31.

39.   Krajka-Kuzniak, V., J. Paluszczak, and W. Baer-Dubowska, Xanthohumol induces phase II enzymes via Nrf2 in human hepatocytes in vitro. Toxicol In Vitro, 2013. 27(1): p. 149-56.

40.   Hwang, Y.J., et al., In vitro antioxidant and anticancer effects of solvent fractions from prunella vulgaris var. lilacina. BMC Complement Altern Med, 2013. 13(1): p. 310.

41.   Jun, M.S., et al., Ethanol extract of Prunella vulgaris var. lilacina inhibits HMGB1 release by induction of heme oxygenase-1 in LPS-activated RAW 264.7 cells and CLP-induced septic mice. Phytother Res, 2012. 26(4): p. 605-12.

42.   Hwang, S.M., et al., Prunella vulgaris Suppresses HG-Induced Vascular Inflammation via Nrf2/HO-1/eNOS Activation. Int J Mol Sci, 2012. 13(1): p. 1258-68.

43.   Xia, N., et al., Prunella vulgaris L. Upregulates eNOS expression in human endothelial cells. Am J Chin Med, 2010. 38(3): p. 599-611.

44.   Islam, M.A., et al., Analgesic and anti-inflammatory activity of Leonurus sibiricus. Fitoterapia, 2005. 76(3-4): p. 359-62.

45.   Ahmed, F., M.A. Islam, and M.M. Rahman, Antibacterial activity of Leonurus sibiricus aerial parts. Fitoterapia, 2006. 77(4): p. 316-7.

46.   Wojtyniak, K., M. Szymanski, and I. Matlawska, Leonurus cardiaca L. (motherwort): a review of its phytochemistry and pharmacology. Phytother Res, 2013. 27(8): p. 1115-20.

47.   Calderon, A.I., et al., LC-DAD-MS-based metabolite profiling of three species of Justicia (Acanthaceae). Nat Prod Res, 2013. 27(15): p. 1335-42.

48.   http://en.wikipedia.org/wiki/Luciferase by Oxyjenn 28 February 2012

49.   Espy, M.J., et al., Real-time PCR in clinical microbiology: applications for routine laboratory testing. Clin Microbiol Rev, 2006. 19(1): p. 165-256.

50.   http://at.promega.com/~/media/Files/Resources/Protocols/Technical%20Bulletins/0/CellTiter%20Glo%20Luminescent%20Cell%20Viability%20Assay%20Protocol.pdf

51.   Mo, C., et al., The Crosstalk Between Nrf2 and AMPK Signal Pathways Is Important for the Anti-Inflammatory Effect of Berberine in LPS-Stimulated Macrophages and Endotoxin-Shocked Mice. Antioxid Redox Signal, 2013.

52.   Strathmann, J., et al., Xanthohumol-induced transient superoxide anion radical formation triggers cancer cells into apoptosis via a mitochondria-mediated mechanism. FASEB J, 2010. 24(8): p. 2938-50.

F) Appendix

F) Appendix

F.1 ABBREVIATIONS

A

ADP	Adenosine diphosphate
AICAR	5-aminoimidazole-4-carboxamide ribonucleotide
AID	Auto inhibitory domain
AMP	Adenosine monophosphate
AMPK	Adenosine monophosphate-activated protein kinase
APS	Ammonium persulphate
ARE	Antioxidant response elements
ARE-LUC	Antioxidant response element luciferase
ATP	Adenosine triphosphate

B

Bach1	BTB and CNC homology 1, basic leucine zipper transcription factor 1
Bach2	BTB and CNC homology 1, basic leucine zipper transcription factor 2
BSA	Bovine serum albumin
BuOH	Butanol

C

CaMKKβ	Calcium/calmodulin-dependent protein kinase kinase-β
CBS	Cystathionine β-synthase
CCD	Charge-coupled devices
CDDO-IM	1[2-Cyano-3, 12-dioxooleana-1, 9(11)-dien-28-oyl]imidazole
cDNA	Complementary DNA
CH_2Cl_2	Dichloromethane
CHO	Chinese hamster ovary cells
CoA	Coenzyme A
Ct	Cycle threshold
Cul3	Cullin 3

D

dd H_2O	Double-distilled water
DDCt	Delta delta Ct
DEPC	Diethylpyrocarbonat
DMEM	Dulbecco's Modified Eagle's Medium
DMSO	Dimethylsulphoxide
DNA	Desoxyribonucleic acid
DNase	Deoxyribonuclease
dNTP	Desoxyribonucleoside triphosphates
DTT	Dithiothreitol

E

E.Coli	Escherichia coli
ECL	Enhanced chemiluminescence
EDTA	Ethylenediaminetetraacetic acid
EGFP	Enhanced green fluorescent protein

F

FSC	Forward Side Scatter
Fwd	Forward

G

GCLC	Glutamate cystein ligase catalytic subunit
GHz	Gigahertz
GLUT4	Glucose transporter type 4
GSK3 β	Glycogen synthase kinase 3 beta

H

H_2O	Water
HO-1	Heme oxygenase 1
HPRT	Hypoxanthine phosphoribosyltransferase

J

JS	*Justicia Secunda*

K

Keap1	Kelch-like ECH-associated protein 1
kHz	Kilohertz

L

LC	*Leonurus Cardiaca*
LKB1	Liver kinase B1
LS	*Leonurus Sibiricus*

M

MAF	Musculoaponeurotic fibrosarcoma
MEF	Mouse embryonic fibroblasts
MeOH	Methanol
$MgCl_2$	Magnesium chloride
min	Minutes
mRNA	Messenger ribonucleic acid

N

NAD(P)H	Nicotinamide adenine dinucleotide phosphate
NaOH	Sodium hydroxide
NQO1	NAD(P)H dehydrogenase, quinone 1
Nrf2	Nuclear factor (erythroid-derived 2)-like 2

O

OWE	Original water extract

P

p-AMPK	Phospho AMPK
PAA	Polyacrylamide
PBS	Phosphate buffer solution
PCR	Polymerase chain reaction
PE	Petroleum ether
PMSF	Phenylmethylsulphonyl fluoride
PV	*Prunella Vulgaris*
PVDF	Polyvinylidene fluoride

Q

qPCR	Quantitative polymerase chain reaction
qRT-PCR	Quantitative real time polymerase chain reaction

R

Rev	Reverse
RNA	Ribonucleic acid
RNase	Ribonuclease
ROS	Reactive oxygen species
RT	Reverse transcriptase
RT-PCR	Real time polymerase chain reaction

S

SDS	Sodium dodecyl sulphate
Ser/Thr kinase	Serine/threonine-specific protein kinase
SSC	Side Scatter

T

TAK1	Transforming growth factor β-activated kinase 1
TBE	Tris/Borate/EDTA
TEMED	N,N,N',N'-tetramethylethylene diamine
tot-AMPK	Total AMPK
TRIS	2-Amino-2-hydroxymethyl-propane-1, 3-diol

U

UV	Ultraviolet

V

V	Volt

X

XN	Xanthohumol

F.2 CURRICULUM VITAE

Personal Data

Date of birth	29.08.1985 at Grieskirchen
Mother	Mag.Pharm. Helga Leitner
Father	Dr. Christian Baldinger

Nationality

Austria

Education

1990-1991	Preschool Schladming
1991-1996	Elementary school Schladming
1996-2005	Abbey Gymnasium Admont musical focus
2005-2006	Homeschool teacher in Ecuador
2006-2013	Study of Pharmacy at University of Vienna

F.3 ACKNOWLEDGEMENTS